Review

M≡E and M=E complexes of iron and cobalt that emphasize three-fold symmetry (E≡O, N, NR)

Caroline T. Saouma, Jonas C. Peters *

Division of Chemistry and Chemical Engineering, California Institute of Technology, Pasadena, CA 91125, United States

Contents

ARTICLE INFO

JCP is grateful to his friend and colleague Professor Harry Gray, who continues to be an inspirational mentor and has made discussions of the electronic structures of metal oxos, imides, and nitrides at once so enjoyable and insightful over the course of the past decade. Happy Birthday Chief!

ABSTRACT

Mid-to-late transition metal complexes that feature terminal, multiply bonded ligands such as oxos, imides, and nitrides have been invoked as intermediates in several catalytic transformations of synthetic and biological significance. Until about ten years ago, isolable examples of such species were virtually unknown. Over the past decade or so, numerous chemically well-defined examples of such species have been discovered. In this context, the present review summarizes the development of 4- and 5-coordinate Fe(E) and Co(E) species under local three-fold symmetry.

© 2011 Elsevier B.V. All rights reserved.

1. Introduction

Multiply bonded species of the late transition metals (M≡E and M=E, where E = O, N, NR, CR) have been postulated as key intermediates in many synthetic and enzymatic transformations [1–8]. These transformations include, for example, olefin epoxidation and aziridination [9–14], C–H bond oxygenation and amination
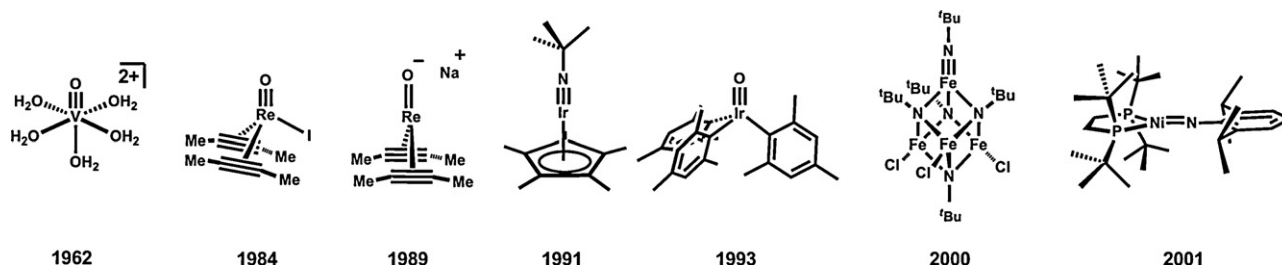
Fig. 1. Examples of M≡E and M=E species, with year of publication noted.

[15–19], and e^-/H^+ transfer processes related to nitrogen fixation [20,21]. The diverse multi-electron reactivity exhibited by such species is in part attributed to their multiple bond character, and there has hence been much interest in understanding the electronic structures and reactivity patterns of such species [22–27].

The molecular orbital (MO) picture of complexes of the type C_{4v}-$L_5M(E)$ was developed in the classic study of the d^1 vanadyl ion (VO^{2+}) by Ballhausen and Gray [28] (Fig. 1). This MO picture stressed a large splitting of the t_{2g} orbitals ($\Delta_\pi \approx 13{,}000\,cm^{-1}$), arising from the presence of a strongly π donating oxo ligand, and the presence of a V≡O triple bond. As a consequence, complexes of the type $L_nM(E)$ should feature *bona fide* multiple bond character, and hence electronic stability, when M(E) π^* orbitals are vacant or only partially filled [1], regardless of local symmetry.

With this generalization in mind, there are at present three well-identified pathways to achieve a reasonable degree of electronic stability in an M≡E or M=E interaction (also abbreviated as M(E)). The most straightforward and hence historically most familiar way is to preserve a low d-electron count at the metal. For a prototypical 6-coordinate metal center that features one terminal multiply bonded ligand $L_5M(E)$, the σ^* and π^* bonding interaction results in the destabilization of four orbitals of d-parentage. It is therefore not surprising that high-valent early transition metals that feature d^0, d^1, or d^2 electron counts have historically dominated the literature of terminal $L_5M(E)$ complexes [29]. To a first order approximation, the π-bond order decreases from 2 to 3/2, 1, and 1/2 as the d^3, d^4, and d^5 configurations are, respectively, populated. Such an approach is of course not limited to complexes of four-fold symmetry. The high stability of complexes such as trigonal bipyramidal (TBP) $\{(Me_3SiNCH_2CH_2)_3N\}V(O)$ [30] and tetrahedral $(^iPr_2N)_3Cr(N)$ [31] drives home this point. A second means of achieving electronic stability in M(E) species constitutes using a combination of ligands that are both σ donating and π-accepting.

Synergism in this context can in principle, via orbital mixing, serve to stabilize d-electrons that would otherwise be destabilized via a strong π^* interaction. Such a scenario has been used, for example, to offer an explanation for the unanticipated stability of the d^6 $L_5Pt(O)$ species prepared by Hill and co-workers [32]. A third mode of achieving electronic stabilization for multiply bonded species is to remove donor ligands from the central metal under consideration. This provides a distinct electronic structure that may be able to accommodate a higher number of d-electrons, so long as those electrons do not fill strongly destabilized orbitals. For example, under three-fold symmetry, both 4- and 5-coordinate species can accommodate M(E) species with diverse d-electron configurations (Fig. 2) [6,27,33–35].

Synthetic entry to M(E) complexes featuring higher d-electron counts first surfaced about 25 years ago when Mayer and Tulip isolated and characterized an intriguing Re(O)I(MeC≡CMe)$_2$ complex (Fig. 1) [33]. This was the first well-characterized terminal M(E) multiple bond linkage for a complex formulated as d^4. The Re–O bond distance of 1.697(3) Å in Re(O)I(MeC≡CMe)$_2$ is similar to that of higher valent Re(O) complexes [36], suggesting that the π^* orbitals are not populated. To achieve such stabilization, the Re adopts a distorted geometry that can be crudely described as tetrahedral, with approximate three-fold symmetry about the Re–O bond [37]. The two electron reduction of a related complex, Re(O)I(PhC≡CPh)$_2$, furnished an equally interesting d^6, 3-coordinate [Re(O)(PhC≡CPh)$_2$][Na] species [35]. In this latter complex, partial population of π^* orbitals is presumed to cause elongation of the Re–O bond to 1.756(3) Å, a destabilization that leads to a more reactive metal center (Fig. 1). At a similar time, Meyer and co-workers identified the interesting intermediate-spin, d^4 ruthenium oxo species (bpy)$_2$(py)Ru(O)$^{2+}$ [38–40]. Again, partial population of π^* orbitals was presumed to give rise to a more reactive Ru(O) linkage.
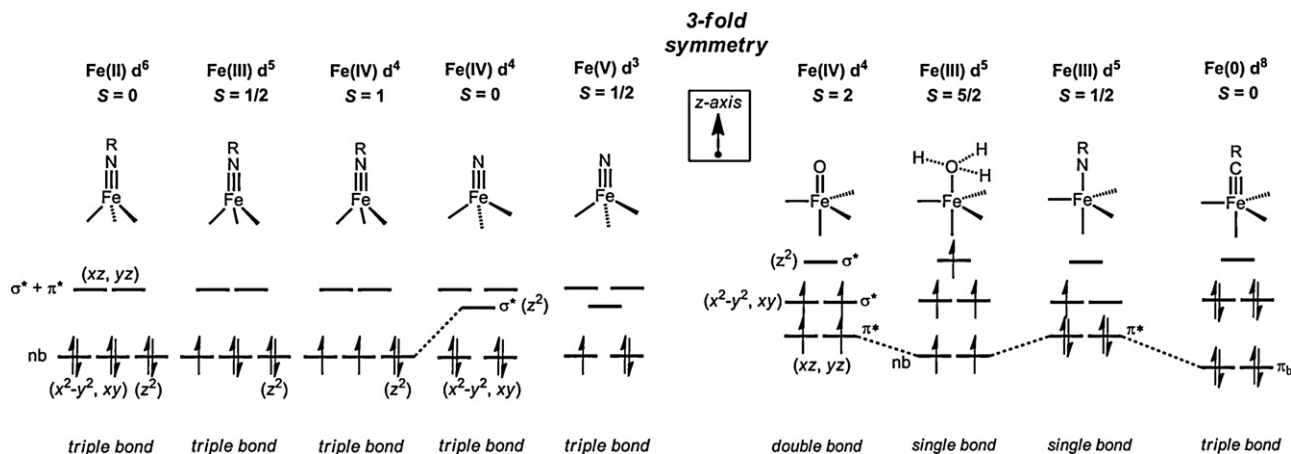

Fig. 2. Qualitative d-orbital splitting diagrams for L_3-Fe(E) and $L'L_3$-Fe(E) structure types discussed throughout the review. The diagram is meant as a guide to the discussion in the text. The relative ordering of the orbital energies for the lower-lying e set (xy, x^2-y^2) and the a_1 orbital (z^2) is not implied for L_3Fe(NR) structures, and are arbitrarily set as degenerate, for simplicity.

By establishing the viability of high d-count structures featuring M(E) bonds, these studies anticipated the possibility that M≡E and M=E complexes of the mid-to-late transition metals might be more generally accessible. Such species would be expected to exhibit the highest degree of kinetic stability for third row ions, and it is hence not surprising that about 15 years ago the groups of Bergman and Wilkinson isolated a d^6 iridium(III) imido complex [41], and a d^4 iridium(V) oxo complex [42], respectively (Fig. 1). Wilkinson's d^4 oxo owes its stability to the fact that its four d-electrons reside in largely non-bonding orbitals that are orthogonal to the Ir–O bond vector. As a consequence of its pseudotetrahedral geometry, its higher energy combined σ^*/π^* orbitals are unfilled.

Until about ten years ago it had been commonly held that, owing to their propensity to populate intermediate and high spin states, first row ions that feature multiply bonded ligands would be highly reactive and hence far more difficult to isolate and thoroughly characterize [1,43–45]. However, this has turned out not to be the case. For example, the ferrocene-like electronic structure of Bergman's Cp*Ir(N^{t}Bu) imide closely resembles that of the isolobal pseudotetrahedral L_3Co(NR) and L_3Fe(NR) imides that are reviewed herein (Fig. 2). Similarly, while the electronic structure of Wilkinson's d^4 iridium oxo was not described at the time of its synthesis, its relative stability predicted the electronic stability of pseudotetrahedral iron nitrides of the type d^4 L_3Fe(N) (Fig. 2).

Indeed, over the past ten years, there have been several reports of Fe [6,27,46–56], Co [57–60], and Ni [61–64] complexes that feature multiply bonded ligands, in both high- and low-spin configurations. In many instances, the coordination number and hence symmetry of the species has been reduced. From these reports a general picture of the electronic structures and reactivity patterns of such complexes is emerging. This article reviews the development of terminal M(E) species of cobalt and iron with a specific emphasis on complexes that reside in local three-fold symmetry. Hillhouse [62–64], Holland [65–68], and Warren [60,61] have advanced the field of 3-coordinate M(E) species in approximate C_{2v} symmetry, though a discussion of these systems is beyond the scope of this review.

2. The L₃M-X structure type

2.1. Electronic lessons learned from pseudotetrahedral cobalt(II)

Prior to delving into a discussion of M(E) species of iron and cobalt, it is instructive to first consider the electronic structures of pseudotetrahedral L_3Co^{II}-X species, as they provided an important lesson with respect to the stabilization of L_3M(E) species. Our group has extensively studied a family of low-spin, high-spin, and spin-crossover complexes of the type L_3Co^{II}-X [69–71], in which the L_3 donor ligand is the anionic tris(phosphino)borate ligand, [PhBP$^R_3$] ([PhBP$^R_3$] = [PhB(CH₂PR₂)₃]⁻; R = Ph, ^{i}Pr) [72,73]. The electronic structure model we proposed to account for the magnetic properties of these pseudotetrahedral d^7 ions provided a useful guide to further consider the stability (or instability) of other d-electron configurations for related structure types, especially where the terminal ligand would be multiply bonded to the metal center.

Prior to the characterization of low-spin [PhBP$^{Ph}_3$]Co^{II}-X complexes, all of the 4-coordinate cobalt(II) systems known to exhibit low-spin ground state configurations were classified as square planar [74]. Ions of approximate tetrahedral geometries, whether of nearly perfect T_d symmetry, or species more appropriately described as pseudotetrahedral, distorted tetrahedral, or trigonal bipyramidal had been, without exception, classified as high-spin [75–78]. A similar situation existed for the well-documented cases of iron(II) and nickel(II) ions. These latter systems had been reported to populate high-spin electronic configurations when

approximately tetrahedral ($S = 2$ and $S = 1$, respectively), and low-spin configurations when square planar [79–81].

The familiar tetrahedral ligand-field for divalent cobalt ions places three degenerate orbitals, the t set, at a significantly higher energy than a nonbonding e set (Fig. 3). This splitting is not generally large enough to enforce a low-spin configuration, and hence a high-spin $S = 3/2$ electronic configuration is typically observed. Lowering the symmetry, whether to C_3, C_s, or C_1, does not typically have a large effect on the relative arrangement of the d-orbitals; the splitting of the degenerate t set is generally small by comparison to the pairing energy that would be required to achieve a low-spin configuration. A strong axial distortion, whereby the angles between three of the ligands decrease to well below 109.5° (as would be enforced by a tripodal ligand), stabilizes the orbital of a_1 symmetry (in C_{3v}) from the upper set by decreasing angular overlap between the L donors and dz^2 [69,71,82,83]. When the ligand-field splitting becomes unusually large, which will be the case for highly covalent, strongly σ-donating and possibly π-accepting L_3 donor sets, a low-spin ground state configuration can be attained (Fig. 3) [69–71].

The d-orbital splitting diagram achieved under this scenario recalls the "two-over-three" splitting commonly used to describe octahedral coordination complexes. A low-spin configuration for a pseudotetrahedral d^7 L_3M-X system is thus expected to exhibit a stabilizing Jahn–Teller distortion, away from three-fold symmetry, to split the upper e set. This distortion attenuates a σ antibonding interaction between a phosphine donor and the metal centered SOMO, and is similar to that observed in pseudo-octahedral low-spin d^7 ions. Such a distortion is evident in the solid-state structures of numerous low-spin [PhBP$^R_3$]Co-X complexes that have been characterized [71], representative examples of which are shown in Fig. 4. The generality of this phenomenon has been probed by comparing the structural and magnetic data for a series of [PhBP$^R_3$]Co-X complexes. Subtle electronic and steric changes, both within the immediate coordination sphere and well removed from it, have been found to affect the spin-state.

The electronic structure depicted in Fig. 3 suggested that removal of a single electron from pseudotetrahedral L_3Co^{II}-X systems might give rise to an $S = 0$ ground state, particularly if significant π donation from the X-type linkage would complement the σ-donor character of the tripodal L_3 scaffold. The complex {[PhBP$^{Ph}_3$]Co^{III}-OSiPh₃}{BPh₄} provided one such case (Fig. 4), and clearly illustrated the close electronic structure relationship that exists between the trigonal ligand-field of 4-coordinate L_3Co^{III}-X complexes and the conventional ligand-field of octahedral L_6Co^{III} species.

Around the time that we were developing the MO description of L_3Co^{II}-X and L_3Co^{III}-X$^+$ complexes, Lee and co-workers reported a tetranuclear iron cluster that featured an Fe(NR) terminal linkage [84]. The iron that coordinates the terminal imido functionality in this system resides in a pseudotetrahedral geometry. Despite the low synthetic yield of the tetranuclear iron cluster (1–2%), they were able to characterize it by several spectroscopic techniques, including X-ray crystallography. Also, Hillhouse and co-workers reported the isolation of a structurally distinct, 3-coordinate nickel imide in 2001 (Fig. 1) [62]. These two results, combined with our electronic structure description for 4-coordinate L_3M-X systems, suggested that a variety of d-electron configurations (i.e. d^3, d^4, d^5, d^6) might be electronically stabilized by strong π-bonding at mid-to-late first row transition ions (Fig. 2).

2.2. Pseudotetrahedral L₃Co(NR) species

Intrigued by the possibility that L_3M(E) species might prove sufficiently stable to isolate, our group began to systematically explore the synthetic feasibility of accessing such complexes. Given
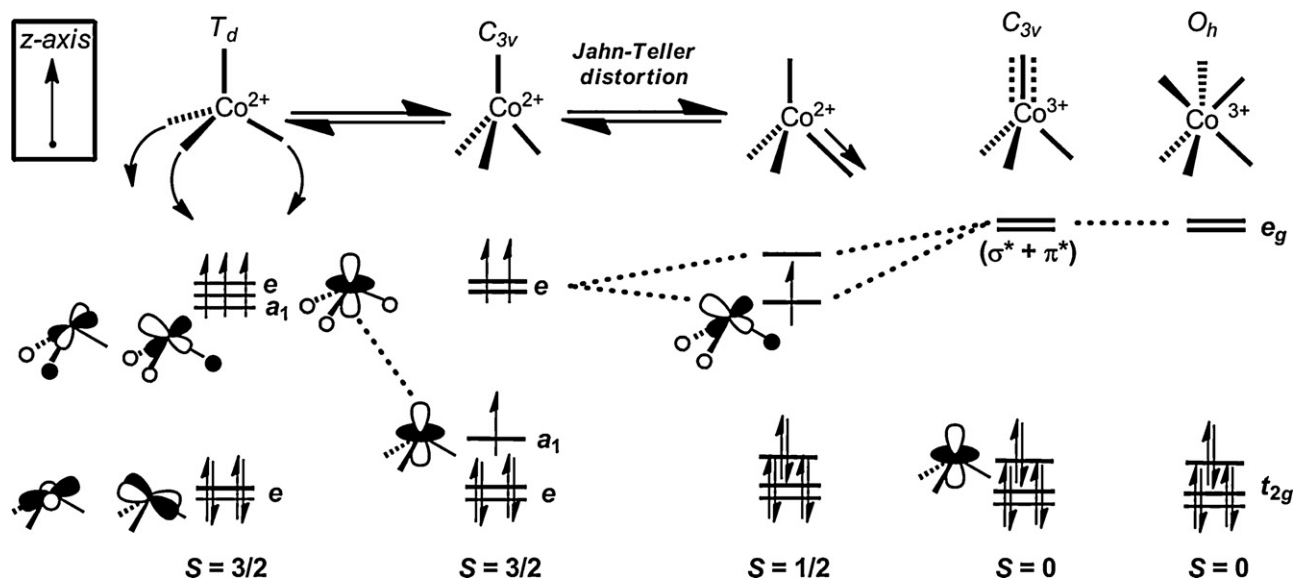
Fig. 3. Qualitative d-orbital correlation diagram that summarizes the electronic relationships discussed in the text regarding 4-coordinate L₃Co-X species.
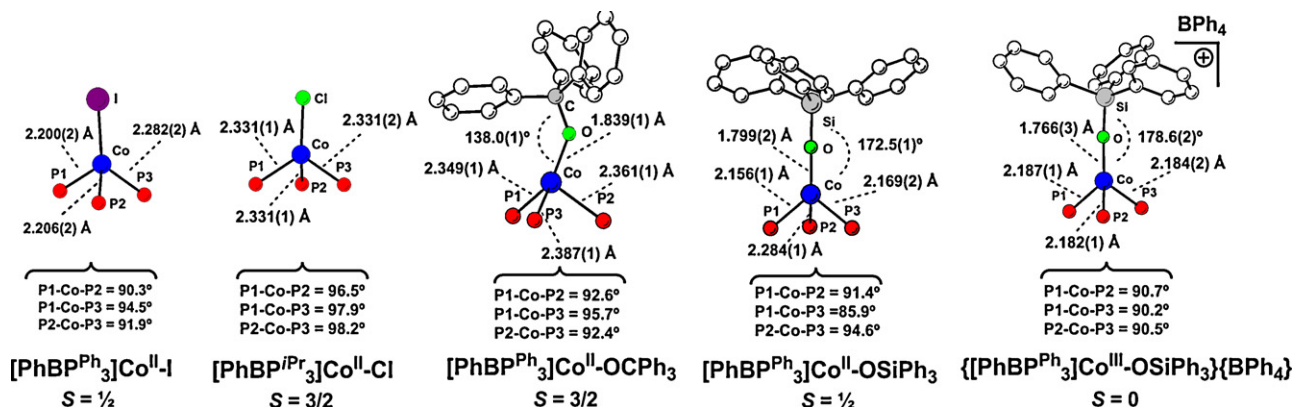

Fig. 4. Select structural data for a series of pseudotetrahedral [PhBP$^R_3$]Co-X species that feature both high- and low-spin ground-states.

our observation that low-spin cobalt(II) systems supported by tris(phosphino)borate ligands were accessible, cobalt(III) seemed like a good place to begin. The soft, polarizable phosphine donors of [PhBP$^R_3$] ligands provided straightforward access to monovalent cobalt(I) precursors of the type [PhBP$^{Ph}_3$]Co^I-L [57]. Subsequent two-electron [NR] group transfer from an organic azide to cobalt proved a reliable means of generating terminal cobalt(III) imides.

This reaction manifold moreover exposed for the first time the viability of a Co$^{III/I}$ two-electron redox couple.

Access to [PhBP$^R_3$]Co^I-L precursors could be accomplished in a two-step sequence starting from a [PhBP$^R_3$]Co^{II}-X precursor via addition of the donor L ligand followed by reduction (Scheme 1) [57,73]. In our initial report, treatment of green [PhBP$^{Ph}_3$]Co^{II}-I with PMe₃ afforded the red 5-coordinate cobalt(II)
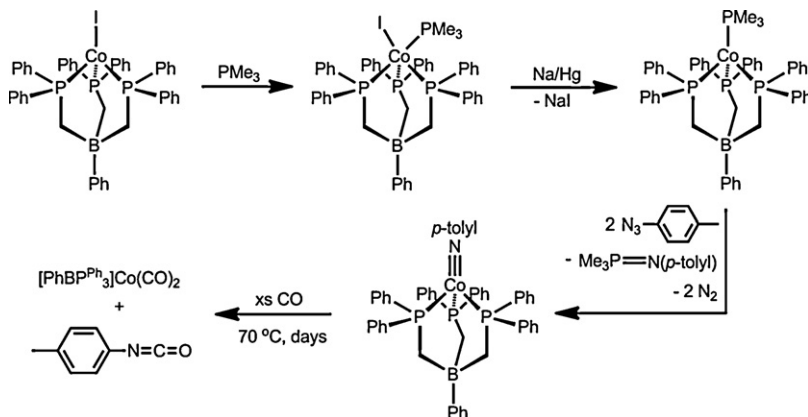
Scheme 1.

Table 1
Select metrical parameters for pseudotetrahedral $L_3Co^{III}(NR)$ complexes.

Complex	Co–N bond length (Å)	N–C bond length (Å)	Co–N–C angle (°)	Displacement of Co from L_3 plane (Å)	Ref.
$[PhBP^{Ph}_3]Co(Np\text{-tolyl})$	1.658(2)	1.367(2)	169.5(1)	1.23	[57]
$[PhBP^{Ph}_3]Co(N^tBu)$	1.633(2)	1.442(2)	176.7(1)	1.24	[85]
$[PhBP^{iPr}_3]Co(Np\text{-tolyl})$	1.667(2)	1.315(3)	173.2(2)	1.21	[73]
$[(TIMEN^{mes})Co(Np\text{-OMeC}_6H_4)][BPh_4]$	1.675(2)	1.386(4)	168.7(2)	0.90	[58]
$(Tp^{tBu,Me})Co(N^tBu)$	1.660(3)	1.449(3)	179.4(3)	1.20	[86]
$(Tp^{tBu,Me})Co(NAd)$	1.655(2)	1.441(3)	178.3(2)	1.196	[87]
$[PhB(^tBuIm)_3]Co(N^tBu)$	1.659(3)	1.463(5)	179.7(3)	1.17	[59]

complex, $[PhBP^{Ph}_3]Co^{II}(I)(PMe_3)$. Reduction by sodium/mercury amalgam then provided the desired bright green cobalt(I) precursor, $[PhBP^{Ph}_3]Co^I\text{-}PMe_3$, as a d^8 $S=1$ species (the two unpaired electrons populate nearly degenerate σ^* orbitals of dxz/dyz parentage). Treatment of $[PhBP^{Ph}_3]Co^I\text{-}PMe_3$ with two equivalents of $N_3(p\text{-tolyl})$ resulted in N_2 extrusion and successful formation of the red and diamagnetic terminal imide $[PhBP^{Ph}_3]Co^{III}(N\text{-}p\text{-}$ tolyl) (Scheme 1). Two equivalents of $N_3(p\text{-tolyl})$ are required in this reaction because one equivalent serves to oxidize PMe_3 to $PMe_3=N(p\text{-tolyl})$.

The solid-state structure of $[PhBP^{Ph}_3]Co^{III}(N\text{-}p\text{-tolyl})$ revealed a very short Co–N bond distance of 1.658(2) Å, establishing the presence of significant multiple bond character at the *Co-NR* linkage [57]. The relatively linear Co–N–C angle of $169.51(2)^\circ$ indicated sp-hybridization at the imide N-atom, establishing two π-bonds between the cobalt and the nitrogen atoms (Table 1). Such a $[PhBP^{Ph}_3]Co^{III}\equiv N(p\text{-tolyl})$ bonding description is consistent with the qualitative d-orbital splitting scenario described above, and was corroborated by DFT calculations [88]. Hence, three low-lying orbitals of dz^2, dxy, and $dx^2\text{-}y^2$ parentage (a_1+e) accommodate six electrons, whereas the σ and π antibonding orbitals of dxz and dyz parentage lie at higher energies (Fig. 3).

Of interest with respect to chemical reactivity was our observation that, despite the high kinetic stability of $[PhBP^{Ph}_3]Co(N\text{-}$ $p\text{-tolyl})$, it was possible to release the imide functionality from cobalt to a nitrene acceptor, thereby regenerating cobalt(I) [57]. For example, addition of CO to of $[PhBP^{Ph}_3]Co^{III}\equiv N(p\text{-tolyl})$ released the free isocyanate $O=C=N(p\text{-tolyl})$, while generating the 5-coordinate dicarbonyl, $[PhBP^{Ph}_3]Co^I(CO)_2$ (Scheme 1). This reaction, and the analogous release of carbodiimides by addition of $C\equiv NR$, have since become a useful diagnostic probe for the presence of imides coordinated to late transition metals [53,67,89,90]. Additionally, it suggested the viability of a catalytic $M^{III/I}$ redox loop (*vide infra*).

Around the time that our studies of $[PhBP^R_3]Co(NR)$ species were underway, Theopold and co-workers were exploring concep-

tually related transformations at substituted tris(pyrazolyl)borate (Tp′) ligated cobalt(I) precursors in the hope of gaining evidence for terminally bonded cobalt imide and oxo functionalities [87,91,92]. Whereas they ultimately established the fidelity of the $L_3Co^{III}(NR)$ framework for certain (Tp′) and NR functionalities, early studies exposed radical degradation pathways. For example, addition of Me_3SiN_3 to $(Tp^{tBu,Me})Co(N_2)((Tp^{R,R'})^- = $ hydrotris(3-R,5-R′-pyrazolyl)borate) resulted in formation of cyclometallated, 5-coordinate $(HB(pz)_2(\kappa^2\text{-}pz'))Co(NHSiMe_3)$ (Scheme 2) [92]. This product in all likelihood formed via H-atom transfer (HAT) from a ligand C–H bond to *in situ* generated $(Tp^{tBu,Me})Co^{III}(NSiMe_3)$. This idea found merit in the reactivity patterns of isolable (Tp′)Co(NR) species (*vide infra*). An example of such a species is $(Tp^{tBu,Me})Co^{III}(NAd)$, prepared by treatment of $(Tp^{tBu,Me})Co(N_2)$ with AdN_3 (Scheme 2) [87,91]. The metrical parameters of the imide functionality in $(Tp^{tBu,Me})Co^{III}(NAd)(Co\text{-}N=1.655(2)$ Å, Co–N–C = 178.3(2)°) are highly similar to those of $[PhBP^R_3]Co^{III}(NR)$ species, establishing their closely related electronic structures (Table 1). $(Tp^{tBu,Me})Co^{III}(NAd)$ exhibits a low-spin d^6 electronic configuration, and hence is diamagnetic even at room temperature in solution. For example, $(Tp^{tBu,Me})Co^{III}(NAd)$ has a well resolved ^{13}C NMR spectrum. But (Tp′) is a weaker field ligand than $[PhBP^R_3]$, which may afford thermal access to open-shell states that would in part explain the propensity of (Tp′)$Co^{III}(NR)$ derivatives to display H-atom abstraction behavior. For example, gentle heating of solutions of $(Tp^{tBu,Me})Co^{III}(NAd)$ resulted in partial insertion of the nitrene into a ligand C–H bond (Scheme 2).

Meyer and Hu extended the generality of the $L_3Co^{III}\equiv NR$ motif and underscored its stability in preference to a 5-coordinate, trigonal bipyramidal $L'L_3Co^{III}(NR)$ structure type using a flexible tris(carbene)amine scaffold, which features a hemi-labile amine donor at the axial position [58]. Once again, oxidative group transfer to cobalt(I) proved the synthetic method of choice. For example, addition of p-tolylazide to trigonal pyramidal $[(TIMEN^R)Co][Cl]$ led to the terminal imide complex $[(TIMEN^R)Co(N\text{-}p\text{-tolyl})][Cl]$
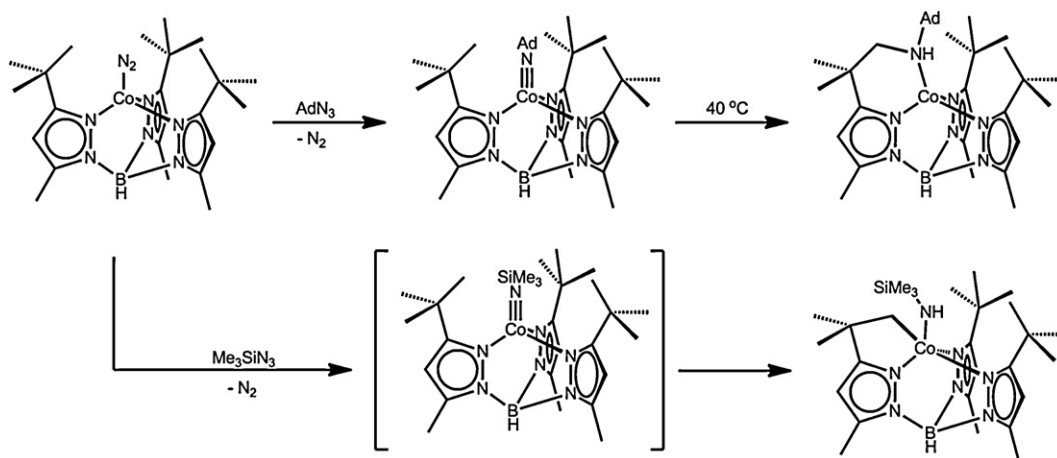
Scheme 2.
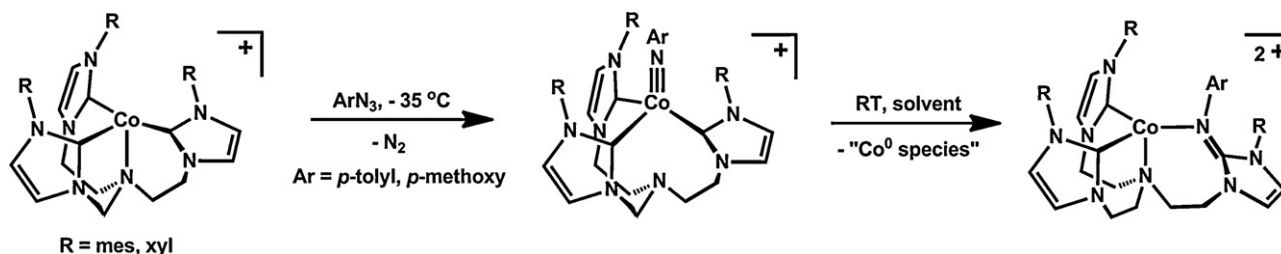
Scheme 3.
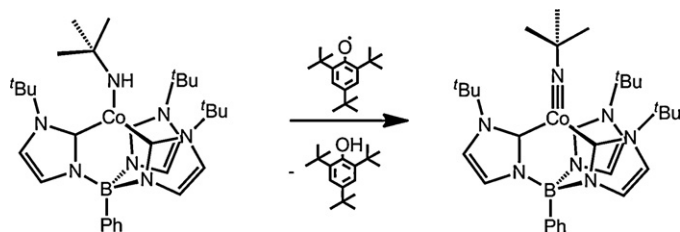
Scheme 4.

(TIMEN^R = tris-[2-(3-R-imidazol-2-ylidene)ethyl]amine; xyl = 2,6-dimethylphenyl; mes = 2,4,6-trimethylphenyl) (Scheme 3). The solid-state structure of the imide complex clearly established the absence of an interaction between the d^6 cobalt center and the amine N-donor of the (TIMEN^{mes}) ligand (the Co–N$_{ax}$ distance is 4.01 Å). Accordingly, complexes of the type [(TIMEN^R)Co(NAr$^{R'}$)][Cl] are low-spin, and feature similar metrical parameters to the cobalt imides described above. Were there an appreciable interaction between the apical N-donor and the cobalt center, a triplet ground state would instead be expected (see discussion below for 5-coordinate d^6 L'L$_3$M(E) species). Despite the clear preference for a low-spin ground state, these [(TIMEN^R)Co^{III}(NAr$^{R'}$)][Cl] imide complexes are thermally unstable and undergo nitrene insertion into one Co–carbene bond at room temperature (Scheme 3). This transformation may be facilitated by the flexible ligand scaffold, as nitrene transfer is accompanied by coordination of the axial amine. Hence, it is cautioned that the reactivity patterns in such systems are not easily correlated with observed ground spin states.

Another cobalt(III) imide system worth noting in the present context comes from Smith and co-workers [59]. Using sterically encumbering tris(carbene)borate ligands that are isomers of the ubiquitous tris(pyrazolyl)borates, they have prepared structurally related L$_3$Co^{III}(NR) species such as [PhB(^{t}BuIm)$_3$]Co(N^{t}Bu) ([PhB(RIm)$_3$] = [PhB(1-R-2-ylidene)$_3$]$^-$). As for tris(pyrazolyl)borate derivatives, vertical bulk is readily accomplished with these ligands, yet they differ by virtue of a stronger ligand field conferred by the carbene donors [93]. The cobalt(III) imides derived from these platforms are electronically similar to those already described (Table 1). Their method of synthesis provided a noteworthy distinction, however (Scheme 4). H-atom abstraction from the cobalt(II) amide precursor, [PhB(^{t}BuIm)$_3$]Co(NH^{t}Bu), was accomplished by addition of 2,4,6-tri(tert-butyl)phenoxy radical to furnish the d^6 cobalt(III) imide, [PhB(^{t}BuIm)$_3$]Co^{III}(N^{t}Bu). This strategy is related to the stepwise oxidation/deprotonation protocol first employed by Hillhouse and Mindiola to prepare a terminal nickel(II)imide [62]. Worth noting is that in all instances, these cobalt(III) imides lack reversible redox couples. Though this is perhaps intuitive for a reduction event, as a d^7 cobalt(II) species would populate a high-lying orbital, the reason why oxidation to a d^5 cobalt(IV) species is not accessible is less obvious (Fig. 3).

2.3. Pseudotetrahedral L$_3$Fe(NR) species

With the aforementioned '[PhBP$^R_3$]Co' chemistry as a backdrop, our group was eager to explore whether related L$_3$Fe(NR) species could be generated and thoroughly characterized. Whereas terminal imido complexes of ruthenium and osmium had been known for many years [94–97], terminally bonded iron imido complexes were essentially unknown. As noted already, Lee and co-workers had provided the singular exception to this statement in 2000 with the low-yielding synthesis of a tetranuclear iron cluster, {ClFe}$_3${N^{t}BuFe}(μ^3-N^{t}Bu)$_4$, that featured a terminal Fe–N^{t}Bu linkage (Fe–N = 1.635(4) Å, Fe–N–C = 178°) [84].

We were fortunate to find that, akin to the mononuclear L$_3$Co(NR) systems, iron(III) imides of the type [PhBP$^R_3$]Fe(NR) were synthetically accessible via two-electron oxidative group transfer to iron(I) precursors [53,73,85,98]. Again, access to well-defined iron(I) synthons was therefore necessary. Despite the paucity of iron(I) complexes at the outset of our studies [99,100], such species proved readily accessible by reduction of [PhBP$^R_3$]Fe^{II}-X precursors in the presence of a coordinating L ligand (e.g., L = PR$_3$ or N$_2$). For example, we initially reported that the sodium/mercury amalgam reduction of the yellow and high-spin (S = 2) complex [PhBP$^{Ph}_3$]FeCl in the presence of PPh$_3$ afforded monovalent, orange and high-spin (S = 3/2) [PhBP$^{Ph}_3$]Fe(PPh$_3$) [53]. As for the related cobalt system, addition of two equivalents of p-tolylazide generated the desired terminal d^5 imide species [PhBP$^{Ph}_3$]Fe(N-p-tolyl), in addition to Ph$_3$P=N(p-tolyl) (Scheme 5). Of particular interest to us was the low-spin ground state of [PhBP$^{Ph}_3$]Fe(N-p-tolyl), further buttressing the electronic structure picture that we had forwarded to account for the low-spin d^7 L$_3$Co^{II}-X and d^6 and L$_3$Co^{III}(NR) systems reviewed above.

As for the cobalt(III) imides, iron(III) imides containing a variety of ancillary organic groups have proven accessible using this methodology (Table 2). These iron(III) imides are generally highly colored and exhibit intense low-energy absorptions that can be assigned as imide-to-iron(III) charge-transfer bands [85]. As would therefore be expected, substitution of an alkylimide for an arylimide greatly reduces the intensity of these transitions, while also increasing the energy at which they are observed. Consistent with this observed blue-shift, the vibrations that are predominantly associated with Fe–N–R stretching character are observed around 1100 cm^{-1} for alkylimides and near 960 cm^{-1} for arylimides. While the alkylimides Fe–N–R stretching mode can be very crudely approximated as a harmonic oscillator, the latter arylimides feature strongly vibrationally coupled Fe–N–C$_{ipso}$ and Fe–N–C$_{ipso}$ modes that cannot be decoupled. The d-orbital electronic structures of these iron(III) imides are well described using arguments originally developed for Cp$_2$Fe$^+$ by Gray and co-workers [101,102].

Akin to the cobalt(III) imides, nitrene transfer to CO also proved to be facile for the iron(III) [PhBP$^R_3$]Fe(NR) imides [53]. For instance, addition of one atmosphere of CO to [PhBP$^{Ph}_3$]Fe^{III}(N-p-tolyl) resulted in formation of O=C=N-p-tolyl and [PhBP$^{Ph}_3$]Fe^I(CO)$_2$. Alternatively, addition of C≡N^{t}Bu released the carbodiimide ^{t}BuN=C=N(p-tolyl). We were moreover able to show that
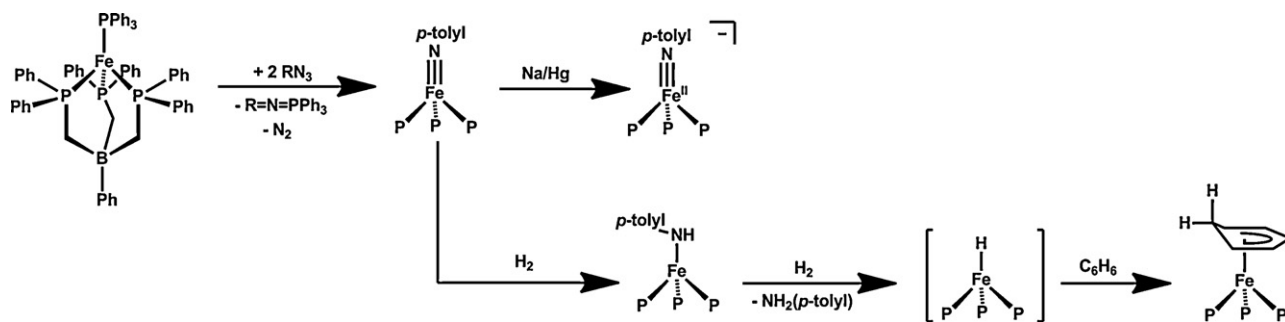
Scheme 5.

the addition of $N_3(p\text{-tolyl})$ to $[PhBP^{Ph}_3]Fe^I(CO)_2$ regenerated $[PhBP^{Ph}_3]Fe(N\text{-}p\text{-tolyl})$, forming the basis for a catalytic nitrene transfer cycle [67].

In addition, the iron imide functionality proved suscepti- ble to hydrogenolysis, a reactivity pattern that Chirik has since reported for a geometrically and electronically distinct iron(III) imide [47]. Treatment of $[PhBP^{Ph}_3]Fe^{III}(N\text{-}p\text{-tolyl})$ with one atmo- sphere of H_2 resulted in complete scission of the Fe–N triple bond, liberating p-tolyl-aniline over the course of days at room tem- perature (Scheme 5) [103]. The high-spin $S = 2$ anilide species, $[PhBP^{Ph}_3]Fe^{II}(HN\text{-}p\text{-tolyl})$, was observed as a long-lived interme- diate and could be isolated. Further exposure to H_2 released $H_2N\text{-}p\text{-tolyl}$ and '$[PhBP^{Ph}_3]Fe(H)$'. The latter hydride species [104] was not observed but inferred from a subsequent benzene inser- tion reaction to generate $[PhBP^{Ph}_3]Fe(\eta^5\text{-}C_6H_7)$. The solid-state structure of $[PhBP^{Ph}_3]Fe^{II}(HN\text{-}p\text{-tolyl})$ showed an Fe–N–C angle of 127.4(2)° and a Fe–N bond distance of 1.913(2) Å, compared with the respective parameters of 170.0(2)° and 1.658(3) Å for $[PhBP^{Ph}_3]Fe^{III}(N\text{-}p\text{-tolyl})$. These distinct metrical parameters estab- lish sp^2-hybridization at nitrogen, which disrupts the degenerate π bonding manifold of the terminally bonded imide precursor. This disruption in turn leads to a preference for a high-spin configura- tion, owing to a weakened ligand field.

According to the qualitative d-orbital electronic structure pic- ture we had advanced for these pseudotetrahedral $L_3M^{III}(NR)$ imides (Figs. 2 and 3), we anticipated that iron(II) imides should also be accessible. We were gratified to observe that treatment of $[PhBP^{Ph}_3]Fe(NAd)$ with one equivalent of sodium/amalgam, fol- lowed by addition of $[^nBu_4N][Br]$, resulted in the clean generation of $\{[PhBP^{Ph}_3]Fe^{II}(NAd)\}\{^nBu_4N\}$ [54]. The metrical parameters of the imide ligand in this d^5 and d^6 redox pair are similar, pre- serving short Fe–N bonds (approximately 1.65 Å) and near linear

Fe–N–C bond angles (Table 2). These observations are consis- tent with a high degree of Fe–N π-bonding. The presence of two strong π-bonds from the imide linkage, along with the strong field tris(phosphino)borate ligands, once again confers the low- spin configuration for the iron(II) system. The electronic structure of $\{[PhBP^{Ph}_3]Fe(NAd)\}\{^nBu_4N\}$ was probed by DFT methods, and is best described by a splitting diagram in which an orbital of $3dz^2$ parentage lies at low energy, close to $3dxy$ and $3dx^2\text{-}y^2$ orbitals that are orthogonal to the Fe–N bond vector. The electronic struc- ture pictures of low-spin $L_3Fe^{II}(NR)^-$, and isoelectronic $L_3Co^{III}(NR)$, are hence closely related to that which was originally elucidated for ferrocene in the classic study by Gray and co-workers nearly four decades ago [102,105].

Fig. 5a plots the visible absorption spectra of select $L_3Fe^{II}(NR)^-$ and $L_3Co^{III}(NR)$ species. If one uses the spin-allowed optical transi- tion assignments (two $^1A_{1g} \rightarrow {}^1E_{1g}$ and one $^1A_{1g} \rightarrow {}^1E_{2g}$) for Cp_2Fe and Cp_2Co^+ as a basis to assign the optical transition assignments for d^6 $L_3Fe(NR)^-$ and $L_3Co(NR)$, then one derives a splitting Δ_1 of ca. 1 eV between the lowest nonbonding $xy/x^2\text{-}y^2$ e-set and the z^2a_1 orbital (Fig. 5b). This splitting is substantially smaller than the splitting Δ_2 of ca. 2 eV between the a_1 orbital and the highest-lying xz/yz e-set that is strongly σ^* and π^* in character. The splitting Δ_1 is not anticipated by ground state DFT calculations of d^6 $L_3M(NR)$ imides, which place the a_1 orbital nearly degenerate with the nonbonding e-set. It would be of obvious interest to theoretically calculate the optical transitions of d^6 $L_3M(NR)$ imides to further explore this issue.

An obvious progression was to next begin exploring whether the d^4 iron(IV) configuration might also be compatible within the $L_3Fe(NR)$ framework. In parallel with our own studies of $L_3Fe^{III}(NR)$ systems, terminally bonded 6-coordinate iron(IV) oxos had begun to emerge as rigorously isolable species, for

Table 2
Select metrical parameters for pseudotetrahedral $L_3Fe(NR)$ complexes.

| Complex	Oxidation state	Fe–N bond length (Å)	N–C bond length (Å)	Fe–N–C angle (°)	Displacement of Fe from L_3 plane (Å)	Ref.
$\{ClFe\}_3\{N^tBuFe\}(\mu^3\text{-}N^tBu)_4$	4+	1.635(4)	–	178.6(3)	–	[84]
$\{[PhBP^{Ph}_3]Fe(NAd)\}\{N^nBu_4\}$	2+	1.651(2)	1.434(3)	178.6(1)	1.24	[54]
$[PhBP^{Ph}_3]Fe(NAd)$	3+	1.641(2)	1.428(3)	176.3(2)	1.32	[54]
$[PhBP^{Ph}_3]Fe(Np\text{-tolyl})$	3+	1.658(3)	1.383(3)	170.0(2)	1.31	[53]
		1.661(3)	1.374(3)	167.3(2)	1.29	
$[PhBP^{Ph}_3]Fe(N^tBu)$	3+	1.635(1)	1.442(2)	179.2(1)	1.29	[85]
$[PhBP^{iPr}_3]Fe(NAd)$	3+	1.638(2)	1.438(3)	176.0(2)	1.27	[73]
$[PhBP^{CH2Cy}_3]Fe(NAd)$	3+	1.622(4)	1.433(6)	176.3(3)	1.24	[98]
$[PhB(mesIm)_3]Fe(NCPh_3)$	3+	1.654(3)	1.473(4)	177.7(3)	1.20	[48]
$[PhB(P^{tBu})(pz)]Fe(NAd)$	3+	1.626(8)	1.33(3)	176(1)	1.27	[55]
		1.634(8)	1.59(3)	170(1)	1.26	
$\{[PhB(P^{tBu})_2(pz)]Fe(NAd)\}\{BArF_{24}\}$	4+	1.61(1)	1.44(2)	174(1)	1.13	[55]
$[PhB(P^{tBu})_2(pz^{Me,Me})]Fe(NAd)$	3+	1.647(8)	1.45(1)	172.2(6)	1.22	[55]
		1.652(8)	1.44(1)	172.4(6)	1.23	
$\{[PhB(P^{tBu})_2(pz^{Me,Me})]Fe(NAd)\}\{BArF_{24}\}$	4+	1.634(4)	1.456(6)	176.3(3)	1.11	[55]
$[PhB(mesIm)_3]Fe(NAd)$	3+	1.625(5)	1.441(7)	177.0(3)	1.13	[50]
$\{[PhB(mesIm)_3]Fe(NAd)\}\{BPh_4\}$	4+	1.618(3)	1.439(5)	176.8(3)	1.15	[50]
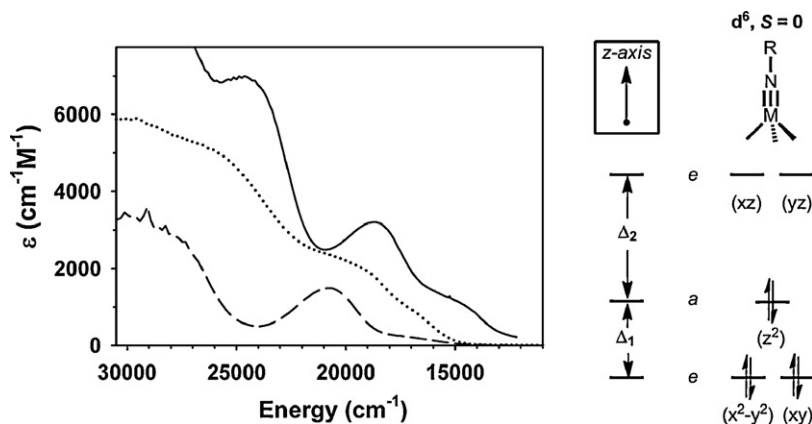
Fig. 5. (a) Visible absorption spectra of d^6 pseudotetrahedral metal imides. All spectra were recorded at room temperature. (A) [PhBP$^{Ph}_3$]Co(NPh) (—); (B) {[PhBP$^{Ph}_3$]Fe(NAd)}$^-$ (...) in THF; and (C) [PhBP$^{Ph}_3$]Co(N^{t}Bu) (– – –). (b) d-orbital splitting diagram defining splittings Δ_1 and Δ_2.

example by the groups of Que and Nam [106–109]. Our initial efforts towards L$_3$Fe^{IV}(NR) species focused on the one-electron chemical oxidation of [PhBP$^R_3$]Fe^{III}(NR) precursors, but we were unsuccessful: if an Fe(IV) species was generated in such reaction mixtures, it was not sufficiently long-lived to be detected by the routine characterization methods we adopted. Interrogation of [PhBP$^R_3$]Fe^{III}(NR) complexes by cyclic voltammetry revealed a chemically irreversible Fe(IV/III) redox couple, contrasting the reversible Fe(III/II) couple that was present at more negative potentials. This observation enforced the notion that [PhBP$^R_3$]Fe^{IV}(NR)$^+$ species are kinetically unstable, and we thus began to explore related 3-coordinate ligand scaffolds in the hopes of lending a higher degree of stability to the iron(IV) state. One path of exploration that ultimately proved efficacious was using hybrid scaffolds, whereby one of the phosphine donor ligands was replaced by a pyrazolyl group. To access such ligands, it proved synthetically necessary to decorate the two phosphine donor arms with *tert*-butyl groups, as the intermediate bis(phosphino)boranes, PhB(CH$_2$PR$_2$)$_2$, were unstable to dimerization when less encumbering groups were employed [110]. Addition of pyrazole anions to PhB(CH$_2$P^{t}Bu$_2$)$_2$ afforded bis(phosphino)pyrazolylborate ligands, abbreviated as [PhB(P^{t}Bu)$_2$(pz$^{R,R'}$)] (pz$^{R,R'}$ = pyrazole substituted at the 3 and 5 positions, respectively).

Using a hybrid scaffold of this type, we found that low-spin terminal iron(III) imides could be readily generated, as for the complexes [PhB(P^{t}Bu)$_2$(pz)]Fe(NAd) and [PhB(P^{t}Bu)$_2$(pz^{Me,Me})]Fe(NAd) [55]. The cyclic voltammograms of these species were distinct from those of tris(phosphino)borate congeners, in that now, the Fe(III/II) couple was irreversible, but the Fe(III/IV) couple was quasi-reversible or reversible at room temperature depending on the scan-rate. Chemical oxidation of these iron(III) imides with [Cp$_2$Fe][BArF$_{24}$] (BArF$_{24}$ = tetra(3,5-di(trifluoromethyl)phenyl)borate) afforded the bright green iron(IV) imides {[PhB(P^{t}Bu)$_2$(pz)]Fe^{IV}(NAd)}{BArF$_{24}$} and {[PhB(P^{t}Bu)$_2$(pz^{Me,Me})]Fe^{IV}(NAd)}{BArF$_{24}$}, the former of which was very thermally unstable (Scheme 6). The Fe–N bond distance in {[PhB(P^{t}Bu)$_2$(pz^{Me,Me})]Fe^{IV}(NAd)}{BArF$_{24}$} is 1.634(4) Å and the Fe–N–C angle is 176.2(3)°, similar to that of all of the pseudotetrahedral iron(III) imides we had characterized. This is consistent with removal of an electron from an orbital that is orthogonal to the *Fe–N*Ad bond vector, and a $(dz^2)^2(dxy)^1(dx^2-y^2)^1(dxz)^0(dyz)^0$ electronic configuration (Fig. 2). Solution Evans method and DFT data were consistent with this $S = 1$ electronic structure picture. Curiously, upon oxidation, the distance between the iron center and the plane defined by the donor atoms of the tripodal ligand (N–P–P) decreased by ca. 0.11 Å to 1.11 Å. This decrease results in slightly longer Fe–P$_{ave}$ bond distances (ca. 0.03 Å) in the iron(IV)

imide compared to the iron(III) congener, which might result in a net decrease of π backbonding from iron into ligand σ* orbitals of appropriate symmetry. This hypothesis is consistent with the observation that the average Fe–P distance decreases by ca. 0.1 Å when neutral [PhBP$^{Ph}_3$]Fe^{III}(NAd) is reduced by one electron to {[PhBP$^{Ph}_3$]Fe^{II}(NAd)}{^{n}Bu$_4$N}, which presumably leads to a net increase in π backbonding into the phosphine ligand σ* orbitals [54].

Smith and co-workers [50] have recently extended the number of well-characterized iron(IV) imides of the pseudotetrahedral L$_3$Fe(NR) structure type via the isolation of an intermediate-spin iron(IV) imide, {[PhB(mesIm)$_3$]Fe^{IV}(NAd)}{OTf}, whose electronic structure is similar to that of {[PhB(P^{t}Bu)$_2$(pz^{Me,Me})]Fe^{IV}(NAd)}{BArF$_{24}$}. This species was generated by oxidation of the precursor iron(III) imide with [Cp$_2$Fe][OTf] (Scheme 6). The metrical parameters for the core atoms of both the iron(III) and the iron(IV) imide congeners are quite similar. For example, the Fe–N$_{imide}$ distances (1.625(4) Å for Fe(III) and 1.618(3) Å for Fe(IV)), the Fe–N–C angle (177.0(3)° for Fe(III) and 176.8(3)° Fe(IV)), and the distance between the iron and the plane defined by the tris(carbene) C-donor atoms (1.13 Å for Fe(III) and 1.15 Å for Fe(IV)) change very little. However, the average Fe–C distance increased by 0.04 Å upon oxidation. Again, diminished π backbonding, in this case into σ* orbitals of the tris(carbene) ligand might offer a plausible explanation.

2.4. Pseudotetrahedral L$_3$Fe(N) species

Well-defined and terminally bound nitrides of iron remain relatively rare. Bridging species are instead often obtained [6,111–114]. Nakamoto and co-workers were first to describe the generation of a terminally bonded iron nitride species using an octaethylporphyrin (OEP) supporting ligand framework [115,116]. They employed a very elegant vibrational analysis to support their assignment. However, the high thermal instability of the (OEP)Fe^V(N) species precluded its further characterization. Wieghardt and co-workers have since characterized low-spin 6-coordinate iron(V) [117,118] and iron(VI) [119] nitrides using cyclam and cyclam-acetate supporting ligands, respectively. These complexes also exhibit limited thermal stability but have been characterized by a suite of spectroscopic techniques, in addition to having been analyzed theoretically [120]. They populate low-spin ground states. The $S = 1/2$ iron(V) d^3 species appears less stable than the diamagnetic iron(VI) species. The latter d^2 species finds close structural and electronic analogy to the well-established and studied Mn(V) nitride systems [12,121,122].
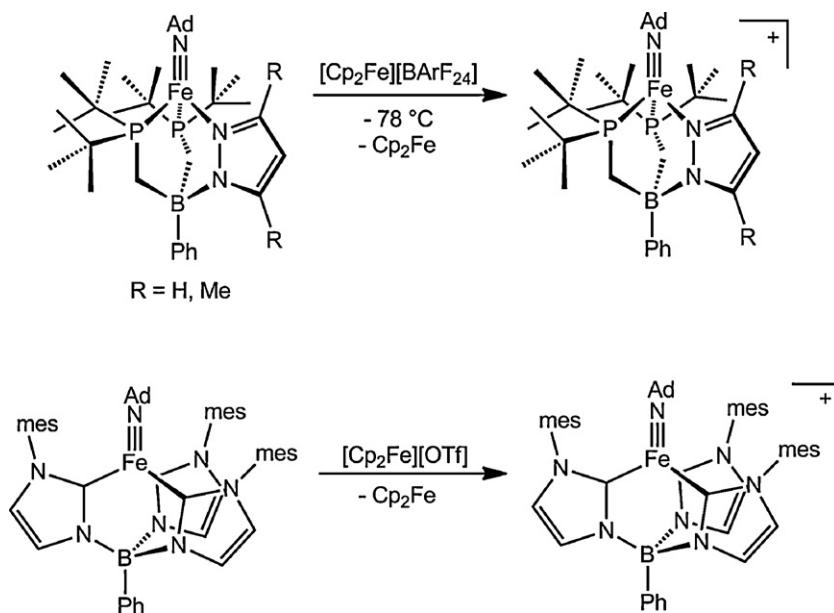
Scheme 6.

Our own group's interest in this area focused instead on exploring the feasibility of terminally bonded nitrides under local three-fold symmetry of the type $L_3Fe(N)$. Theoretical analysis suggested to us that replacement of the terminal NR^{2-} ligand by an N^{3-} ligand in systems of this type would strongly destabilize the a_1 orbital of dz^2 parentage that is low-lying in $L_3Fe^n(NR)$ (n = II, III, IV) species (Fig. 2) [52]. Such destabilization would thereby render d^5 and d^6 configurations comparatively less favorable due to population of a strongly antibonding σ^* orbital. By contrast, d^4 and perhaps even lower d-count species might be electronically favored, as there are only two energetically low-lying d-orbitals (dx^2-y^2/dxy). For an iron(IV) species, the predicted electronic configuration is therefore $(xy)^2(x^2$-$y^2)^2(z^2)^0(xz)^0(yz)^0$ (Fig. 6). Such a configuration is similar to Wilkinson's d^4 $Mes_3Ir(O)$ complex. The destabilization of dz^2 relative to the structurally related imides is a consequence of better overlap with the nitrogen sp-hybrid orbital, and a distortion that renders the geometry about the iron center more tetrahedral. The

calculated S = 0 $[PhBP^{iPr}_3]Fe(N)$ structure features P–Fe–P angles between 99° and 101°, whereas these calculated angles for the corresponding imide, S = 0 $\{[PhBP^{iPr}_3]Fe(N^tBu)\}^-$, are between 90° and 95°, in accord with a wealth of experimental data. It was therefore incumbent upon us to select an appropriate N-atom transfer agent to test whether an S = 0 nitride would be accessible using the tris(phosphino)borate iron frameworks.

Nitride transfer reactions often occur as two-electron processes that deliver an N-atom while liberating a thermodynamically stable molecule. Azide, N_3^-, is often the reagent of choice owing to its synthetic simplicity and the release of N_2 as a byproduct [49,51,115,117,123]. N_2 extrusion can occur spontaneously or it can be effected by heating or photolytic means, the latter often being necessary when the resultant nitride is thermally unstable. We found that such protocols were ineffective for generating terminal nitrides with the '$[PhBP^{iPr}_3]Fe$' and '$[PhBP^{Ph}_3]Fe$' frameworks. For example, $\{[PhBP^{Ph}_3]Fe(N_3)\}_2$ can be prepared and is a thermally stable species. While N_2 extrusion might have been effected by its one-electron reduction to release the d^5 $\{[PhBP^{Ph}_3]Fe(N)\}^-$ and N_2, any such species appears to be rapidly trapped by "$[PhBP^{Ph}_3]Fe^I$" in solution (iron(I) is generated by kinetically competitive loss of N_3^-

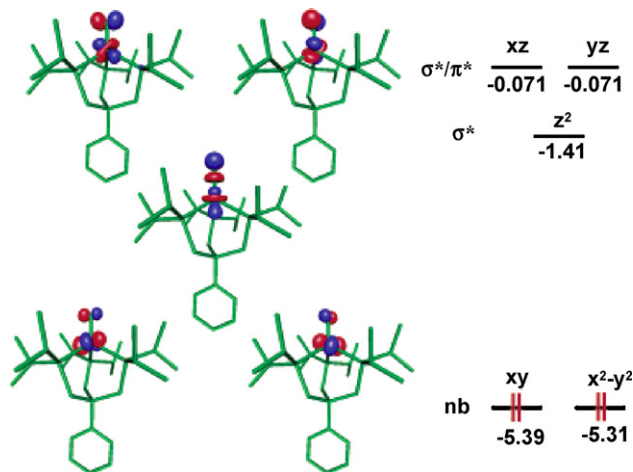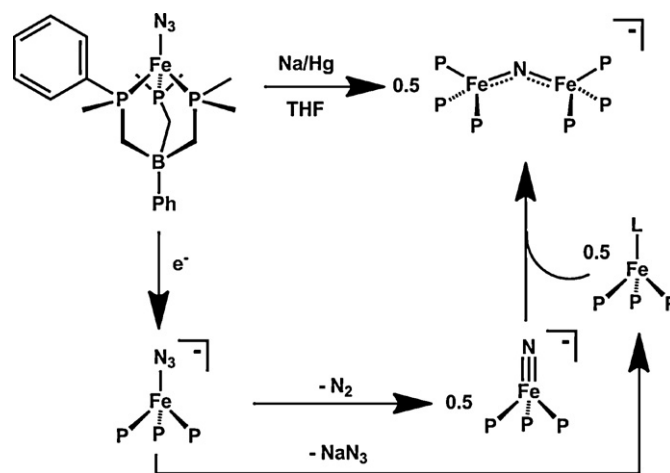**Fig. 6.** Theoretically predicted geometry and electronic structure (DFT, JAGUAR 5.0, B3LYP/LACVP**) for S = 0 $[PhBP^{iPr}_3]Fe≡N$. Lobal representations correspond to the frontier orbitals (energies in eV). Structural parameters: Fe–P = 2.28, 2.28, 2.29 Å; N–P–Fe = 117, 117, 119°; P–Fe–P = 99, 101, 101°; Fe–N = 1.490 Å.
Source: Reprinted with permission from ref. [52]. Copyright 2004 American Chemical Society

Scheme 7.
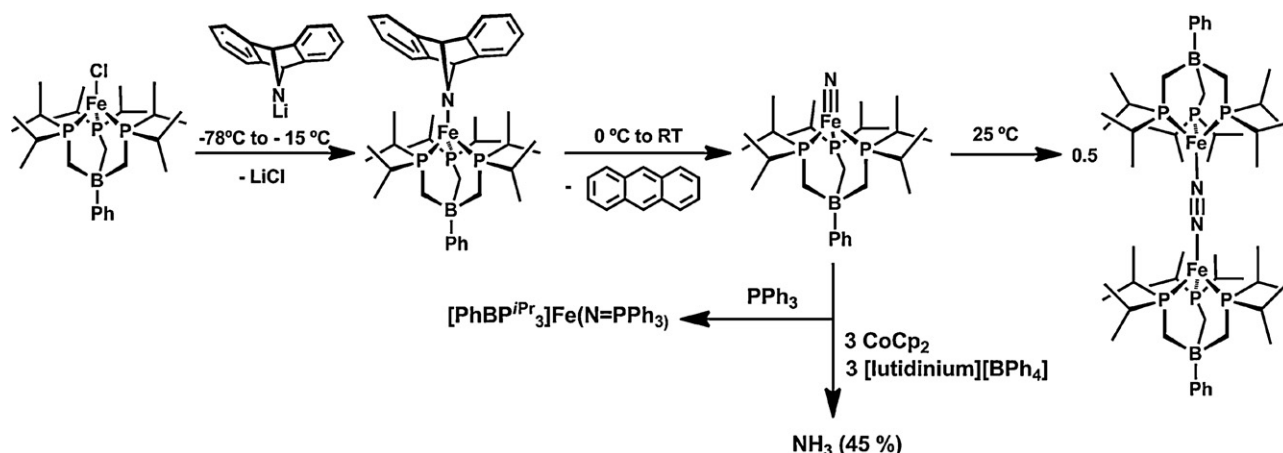
Scheme 8.

Table 3
Select spectroscopic and structural parameters of pseudotetrahedral $L_3Fe^{IV}(N)$ complexes.

Complex	Fe–N stretch $^{14}N/^{15}N$ (cm^{-1})	Fe–N distance (Å)	Displacement of Fe from L_3 plane (Å)	^{15}N NMR chemical shift[a] δ	MB δ (mm s^{-1})	MB $\Delta E_Q \delta$ (mm s^{-1})	Ref.
[PhBP$^{iPr}_3$]FeN	1034/1007	1.51–1.54[b]	–	952	−0.34(1)	6.01(1)	[52,131,132]
[PhBP$^{CH2Cy}_3$]FeN	–	1.55[b]	–	929	−0.34(1)	6.01(1)	[131,132]
[(TIMEN^{mes})FeN][BPh$_4$]	1008/982	1.526(2)	0.43	1121	−0.27(1)	6.04(1)	[51]
[(TIMEN^{xyl})FeN][BPh$_4$]	–	1.527(3)	0.38	–	–	–	[51]
[PhB(^{t}BuIm)$_3$]FeN	1028/999	1.512(1)	0.98	1019	–	–	[49]
[PhB(mesIm)$_3$]FeN	–	1.499(5)	1.01	1004	–	–	[48]

[a] Referenced to liquid NH$_3$ at 0 ppm.
[b] Obtained by EXAFS.

upon reduction) to afford the stable diiron(II) μ-nitride complex $\{[PhBP^{Ph}_3]Fe\}_2(\mu\text{-}N)^-$, as shown in Scheme 7 [54].

An alternative approach that proved viable involved use of the N-atom transfer agent Li(dbabh) (dbabh = 1,2:5,6-dibenzo-7-aza bicyclo [2.2.1]hepta-2,5-diene). This lithium amide was first used by Cummins and Mindiola to prepare a high-valent chromium nitride [124]. Its utility involves initial formation of a metal amide, M^n-(dbabh), which can thermally release $M^{n+2}(N)$ and one equivalent of anthracene. The utility of this reagent appears to be limited; for example, we have explored its use to install nitride groups at '[PhBP$^R_3$]Mn' and '[PhBP$^R_3$]Ni' systems and in doing so have uncovered alternative reaction manifolds [125,126]. But to our satisfaction (and relief!), the synthon worked well for '[PhBP$^{iPr}_3$]Fe'.

Using Li(dbabh), the iron(IV) nitride species, [PhBP$^{iPr}_3$]Fe^{IV}(N), can be generated and thoroughly characterized (Scheme 8) [52]. Treatment of [PhBP$^{iPr}_3$]FeCl with Li(dbabh) at −35 °C generated the red and thermally unstable iron(II) amide intermediate, [PhBP$^{iPr}_3$]Fe^{II}(dbabh). Upon warming to 0 °C, this intermediate underwent clean first order decay to release one equivalent of anthracene and the desired diamagnetic product, [PhBP$^{iPr}_3$]Fe(N). Owing to its many spin active nuclei and its diamagnetism, solution NMR characterization of [PhBP$^{iPr}_3$]Fe(N) was straightforward. For example, a diagnostic ^{15}N NMR chemical shift of 952 ppm was observed for the nitride (Table 3), in accordance with the chemical shift noted for terminal M(N) species [31,127–129]. The solution IR spectrum showed an Fe–N stretch at 1034 cm^{-1} which is consistent with that of other M(N) species [130]. Upon ^{15}N-labelling, the stretch shifts to 1007 cm^{-1}, in agreement with that calculated (27 cm^{-1}) assuming an Fe–N harmonic oscillator. The Mössbauer spectrum of [PhBP$^{iPr}_3$]Fe(N) was also obtained, and established an isomer shift of δ −0.34 mm/s, and an unusually large quadrupole-splitting parameter, $\Delta E_Q = 6.01$ mm s^{-1} [131]. This large quadrupole splitting results from the highly anisotropic electric field gradient that arises from electronic population of dx^2-y^2 and dxy orbitals orthogonal to the B–Fe–N vector, and

has proven diagnostic of $L_3Fe^{IV}(N)$ species (*vide infra*). Spontaneous nitride coupling to generate the formal diiron(I) product, $\{[PhBP^{iPr}_3]Fe\}_2(\mu\text{-}N_2)$, occurred upon concentration or attempts to crystallize [PhBP$^{iPr}_3$]Fe≡N [52]. We canvassed one other scaffold, '[PhBP$^{CH2Cy}_3$]Fe' (CH$_2$Cy = cyclohexylmethyl) and successfully generated and characterized [PhBP$^{CH2Cy}_3$]Fe(N) at low temperature [131]. Though nitride coupling does not occur for this latter system ($\{[PhBP^{CH2Cy}_3]Fe\}_2(\mu\text{-}N_2)$ is *not* an accessible species [98]), [PhBP$^{CH2Cy}_3$]Fe(N) proved to be unstable above −50 °C, and poorly defined degradation pathways frustrated our ability to crystallize this species. Additionally, a short Fe–N bond distance of 1.53(2) Å was obtained for these species by EXAFS [132].

The respective groups of Meyer and Smith have also targeted terminally bonded iron(IV) nitrides in recent years using the carbene ligand frameworks introduced above. Meyer's 4-coordinate nitrides, [(TIMEN^R)Fe(N)][BPh$_4$] (R = mes, xyl), formed via photolysis of 4-coordinate azide precursors, [(TIMEN^R)Fe(N$_3$)][BPh$_4$], proved thermally stable and hence amenable to single crystal XRD characterization (Scheme 9) [51]. Such data revealed an Fe–N$_{nitride}$ bond distance of 1.526(2) Å for [(TIMEN^{mes})Fe(N)][BPh$_4$] (Table 3). This complex represented the first reported terminal iron nitride species to be characterized by X-ray crystallography. Smith's X-ray structure of [PhB(^{t}BuIm)$_3$]Fe(N) followed soon
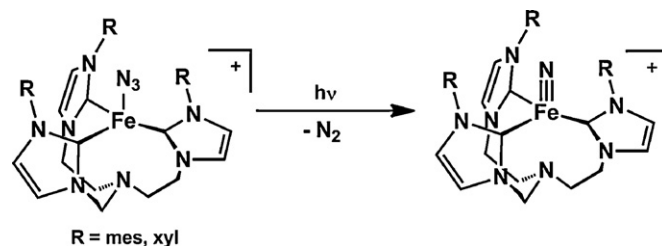
Scheme 9.
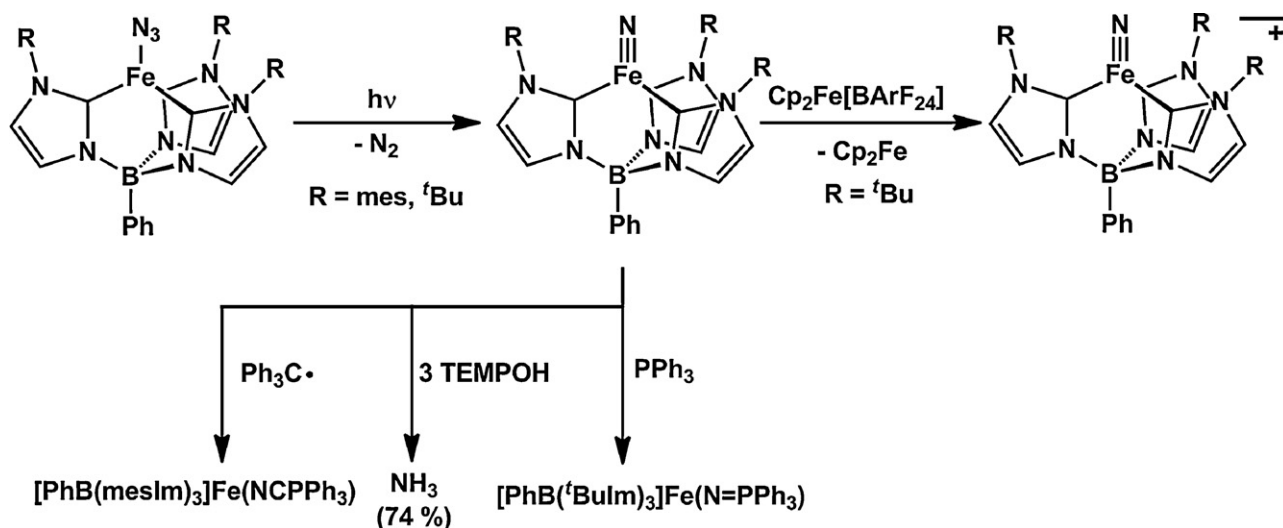
Scheme 10.

thereafter [49]. Meyer's system provided experimental validation that a 4-coordinate $L_3Fe^{IV}(N)$ system is energetically preferred relative to a corresponding 5-coordinate $L'L_3Fe^{IV}(N)$ under local three-fold symmetry, since the apical amine donor does not bind the iron center. The geometry about the iron centers in $[(TIMEN^R)Fe(N)][PPh_4]$ are close to trigonal pyramidal, with the iron centers ca. 0.4 Å above the plane defined by the three carbene donors. The related $[PhB(RIm)_3]Fe(N)$ system reported by Smith and co-workers was likewise generated via photolysis of terminal azide precursors (Scheme 10). As noted for the calculated structure of $[PhBP^{iPr}_3]Fe(N)$, $[PhB(^tBuIm)_3]Fe(N)$ is somewhat more tetrahedral in structure compared to the corresponding iron(IV) imides (i.e., $\{[PhB(^tBuIm)_3]Fe(NAd)\}\{OTf\}$), as the average C–Fe–C angle increases from ca. 90° to ca. 96°. DFT calculations on the iron(IV) nitrides supported by the three different ligand scaffolds indicate similar electronic structures [49,51,52]. Hence, in all three scaffolds the tridentate L_3 donor adopts a geometry such that the a_1 orbital is destabilized to accommodate a favorable d^4 $S = 0$ $(xy)^2(x^2-y^2)^2(z^2)^0(xz)^0(yz)^0$ electronic configuration. Note that this electronic structure is distinct from the iron(IV) imides, which adopt an $S = 1$ ground state due to the fact that the a_1 orbital of dz^2 parentage lies much closer in energy to the nonbonding dxy, dx^2-y^2 e set of orbitals (Figs. 2 and 6).

While the reactivity patterns of these iron(IV) complexes have not been reported in great detail, there are a few transformations worthy of note (Schemes 8 and 10). Treatment of both $[PhBP^{iPr}_3]Fe(N)$ and $[PhB(^tBuIm)_3]Fe(N)$ with triphenylphosphine effected reductive nucleophilic attack and afforded the corresponding high-spin iron(II) phosphiniminato complexes, $[PhBP^{iPr}_3]Fe(N=PPh_3)$ and $[PhB(^tBuIm)_3]Fe(N=PPh_3)$, respectively [49,52]. Our own group was interested in determining whether the terminal nitride of $[PhBP^{iPr}_3]Fe(N)$ could liberate NH_3 on treatment with an e^-/H^+ source, a transformation motivated by a hypothetical Fe-mediated distal scheme for N_2 reduction. It was found that NH_3 could be liberated upon addition of [lutidinium][BPh_4] in the presence of CoCp_2, albeit in moderate yield (ca. 45%) [52]. Smith's nitride, $[PhB(mesIm)_3]Fe(N)$, was treated with a well-defined H-atom transfer equivalent, TEMPOH, and gave rise to an appreciably higher yield of NH_3 (74%) (TEMPOH = 1-hydroxy-2,2,6,6-tetramethylpiperidine) [48]. The first step of this transformation is thought to occur via H-atom transfer (HAT) from TEMPOH to the nitride, though a protonation/reduction mechanism could not be ruled out from the measured free energy of activation. Smith's nitride was also exposed to trityl radical to generate the corresponding iron(III) imide, $[PhB(^tBuIm)_3]Fe(NCPh_3)$. This transformation thereby established another synthetic route to iron imide species.

Perhaps the most interesting reaction to note concerns oxidation of $[PhB(^tBuIm)_3]Fe(N)$. According to the d-orbital configuration proposed for $L_3Fe^{IV}(N)$ species, d-electron configurations less than d^4 should in principle also show electronic stability. Removal of one electron to generate a d^3 $L_3Fe^V(N)$ species is therefore of paramount interest. Such a reaction has very recently been demonstrated using the $[PhB(^tBuIm)_3]Fe(N)$ precursor. Low temperature oxidation by $[Cp_2Fe][BArF_{24}]$ was used to generate the d^3 iron(V) nitride $\{[PhB(^tBuIm)_3]Fe(N)\}\{BArF_{24}\}$, a low-spin species that proved sufficiently stable to isolate and characterize by X-ray crystallography [133]. As should be expected for an $(xy)^2(x^2-y^2)^1(z^2)^0(yz)^0$ $(xz)^0$ electronic configuration, the Fe–N distance remains virtually unchanged (Fe–N = 1.506(2) Å) relative to its d^4 precursor, and the iron center remains ca. 1 Å above the L_3 donor plane. Also, $\{[PhB(^tBuIm)_3]Fe(N)\}\{BArF_{24}\}$ likewise affords a diagnostic large quadrupole splitting parameter $\Delta E_Q = 4.25\ mm\ s^{-1}$ in the Mössbauer spectrum.

3. Trigonal bipyramidal (TBP) $L'L_3$-M(E) structure types

3.1. Orbital considerations

An interesting question that follows the preceeding discussion of $L_3M(NR)$ and $L_3M(N)$ species concerns how the electronic structure rules will vary upon coordination of a fifth ligand in the site *trans* to the multiply bonded ligand E. Such coordination preserves local three-fold symmetry and leads to an $L'L_3M(E)$ structure type, where the L_3 donor set moves into the equatorial plane and L' and E occupy axial sites. Qualitative d-orbital splitting diagrams that provide a starting point for discussing $L'L_3M(E)$ species are shown in Fig. 7. This electronic picture was briefly introduced in a review article by Miskowski et al. [134]. Assuming a σ-only bonding picture, the dxz/yz e set is stabilized by the absence of any σ* interactions with the $L'L_3$ donor set, which contrasts the strongly destabilized σ* dxz/yz e set in pseudotetrahedral $L_3M(E)$ structures. As the E ligand p_x and p_y orbitals are of π symmetry, they can therefore strongly overlap with the dxz/yz e set. If these p-orbitals and the dxz and dyz orbitals are each filled with electron pairs, as they would be in a hypothetical species such as $S = 0$ $L'L_3Fe^{IV}(N)$, then a destabilizing π* interaction is present that removes net π bonding at the Fe–N linkage. By contrast, if the ligand E has empty π acceptor orbitals
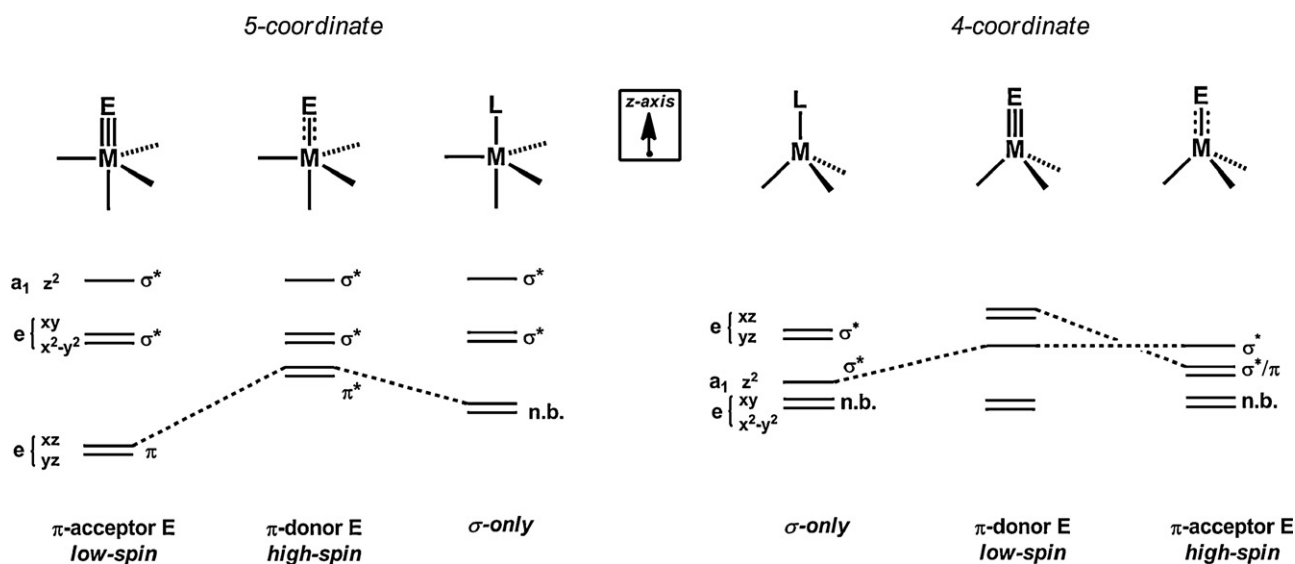
5-coordinate　　　　　　　　　　　　　　　　　　　4-coordinate

Fig. 7. Qualitative d-orbital splitting diagrams for 4- and 5-coordinate C_{3v} species, with the anticipated spin-state for each M(E) type noted.

(akin to a CO or NO$^+$ ligand, for example) then backbonding inter-actions will occur to stabilize the dxz/yz e set and lead to favorable metal-to-E multiple bonding. A degree of favorable net π-bonding can also be achieved even in the case of π-donating ligands such as oxos, imides, and nitrides if only partial population of the dxz/yz e set occurs. Perhaps counter-intuitively, the situation can there-fore arise where a high-spin d-electron configuration can feature greater multiple bond character than an intermediate- or low-spin configuration for L'L$_3$Fe(E) structure types (see Figs. 2 and 7). This may be, for example, achieved using supporting ligands that confer a weak ligand field such that a high-spin state is conferred. This scenario directly contrasts that of L$_3$M(E) species, where high-spin configurations will always attenuate the degree of M(E) π bonding. Below we discuss select and pedagogically informative examples of each of these cases, beginning with systems that tend towards low-spin configurations.

3.2. Trigonal bipyramidal L'L$_3$Fe(NR) species

The well-studied pseudotetrahedral L$_3$Fe^{III}NR complexes fea-ture *bona fide* Fe≡NR triple bonds resulting from two highly destabilized, unoccupied $\sigma^*\pi^*$ orbitals (Figs. 2 and 7). Introducing a ligand *trans* to the imido group and shifting the Fe into the L$_3$ plane of a TBP leads in principle to population of the π^* set, thereby obliterating a significant degree of the Fe–N multiple bonding character presumed responsible for the stability of pseudotetrahe-dral L$_3$Fe^{III}NR species. Accordingly, until very recently metal-ligand multiply bonded species in TBP configurations of the general type L'L$_3$M(E), where E is a prototypical π-donor ligand, had been iso-lated only for d-electron counts of 0 or 1 [26]. TBP systems with higher d-electron counts would be expected to dissociate the api-cal ligand and distort towards the more stable pseudotetrahedral geometry when accommodating an axial metal-ligand multiple bond, as evident from Meyer's nitrides [(TIMEN^R)Fe(N)][BPh$_4$] [51] and imides [(TIMEN^R)Co(NAr)][BPh$_4$] [58].

To explore a system where such distortion of the axial lig-and is prohibited, our group began to study the feasibility of L'L$_3$Fe(E) species using an anionic tris(phosphino)silyl ligand, (2-R$_2$PC$_6$H$_4$)$_3$Si$^-$ ((SiP^R$_3$); R = Ph or ^{i}Pr), as the L'L$_3$ tetradentate scaffold [135,136]. These ligands feature a strongly bound silyl donor in the axial position of a TBP, and three tightly chelated phos-phine donors in the equatorial plane. Using this ligand scaffold, we have recently mapped the synthetic feasibility of iron imides of

the type (SiP^R$_3$)Fe(NR) for direct comparison to [PhBP$_3$]Fe(NR) and related 4-coordinate imides.

In contrast to the [PhBP^R$_3$]$^-$ ligand, which accommodates iron in both high- and low-spin configurations depending on the apically bound ligand (e.g., S = 3/2 [PhBP^{Ph}$_3$]Fe(PPh$_3$) and S = 1/2 [PhBP^{Ph}$_3$]Fe(N^{t}Bu)), the (SiP^R$_3$)$^-$ ligand appears to exclu-sively enforce low- and intermediate-spin configurations. Hence, 5-coordinate iron(I) d^7 (SiP^R$_3$)Fe–L complexes are S = 1/2, as for the representative complexes (SiP^R$_3$)Fe–N$_2$ and (SiP^R$_3$)Fe(PMe$_3$). Similarly, iron(II) d^6 complexes of the type {(SiP^R$_3$)Fe–L}$^+$ and (SiP^R$_3$)Fe–X (L = NH$_3$, N$_2$; X = Cl, Me) are invariably intermediate-spin S = 1. Removal of an additional electron, as for the complex {(SiP^R$_3$)Fe^{III}–Cl}{BArF$_{24}$}, again results in a d^5, S = 3/2 intermediate-spin configuration [135–137].

Using a synthetic protocol analogous to that described for the generation of [PhBP^R$_3$]M^{III}(NR) complexes (M = Fe, Co), we explored the generation of (SiP^R$_3$)Fe(NR) [89]. Our study showed that (SiP^{iPr}$_3$)Fe(NAr) species could be generated by addition of ary-lazides to (SiP^{iPr}$_3$)Fe–N$_2$, but that they were unstable to subsequent decay pathways (Scheme 11). The azide adduct intermediates were more thermally stable and could be isolated for bulky alkyl azide derivatives, for example, (SiP^{iPr}$_3$)Fe(η^1-N$_3$Ad). The dominant decay pathway we have discerned for the (SiP^{iPr}$_3$)Fe(NAr) imide species concerned bimolecular 'NAr' coupling to generate azoarenes ArN=NAr. Such a pathway regenerated (SiP^{iPr}$_3$)Fe^I–N$_2$, and hence arylazides could be catalytically degraded to the azoarene byprod-ucts. Chemical trapping experiments were used to further corroborate the presence of the terminal imide moiety. For exam-ple, addition of ^{t}BuNC released the carbodiimide ^{t}BuN=C=N-p-tolyl and (SiP^{iPr}$_3$)Fe(CN^{t}Bu). This two electron nitrene transfer is diag-nostic of isolable FeNR species (*vide supra*). Also, H-atom trapping by 9,10-dihydroanthracene afforded the d^6 anilide (SiP^{iPr}$_3$)Fe(HN-p-tolyl). Related HAT chemistry has been observed in high-spin 4-coordinate FeNR species [65,138] and invoked in other systems [45]. The ability of (SiP^{iPr}$_3$)FeNAr to facilitate one-electron (HAT), two-electron (nitrene transfer), and four-electron (azoarene for-mation) transformations has hence been demonstrated.

Direct detection of S = 1/2 [SiP^{iPr}$_3$]Fe(N-p-tolyl) was accom-plished using low temperature EPR spectroscopy via *in situ* photolysis of the azide adduct precursor, (SiP^{iPr}$_3$)Fe(N$_3$-p-tolyl), in a frozen glass [89]. These data, in addition to an accompany-ing DFT study, placed a majority of the unpaired spin density on iron for (SiP^{iPr}$_3$)Fe(N-p-tolyl). A distortion away from three-fold
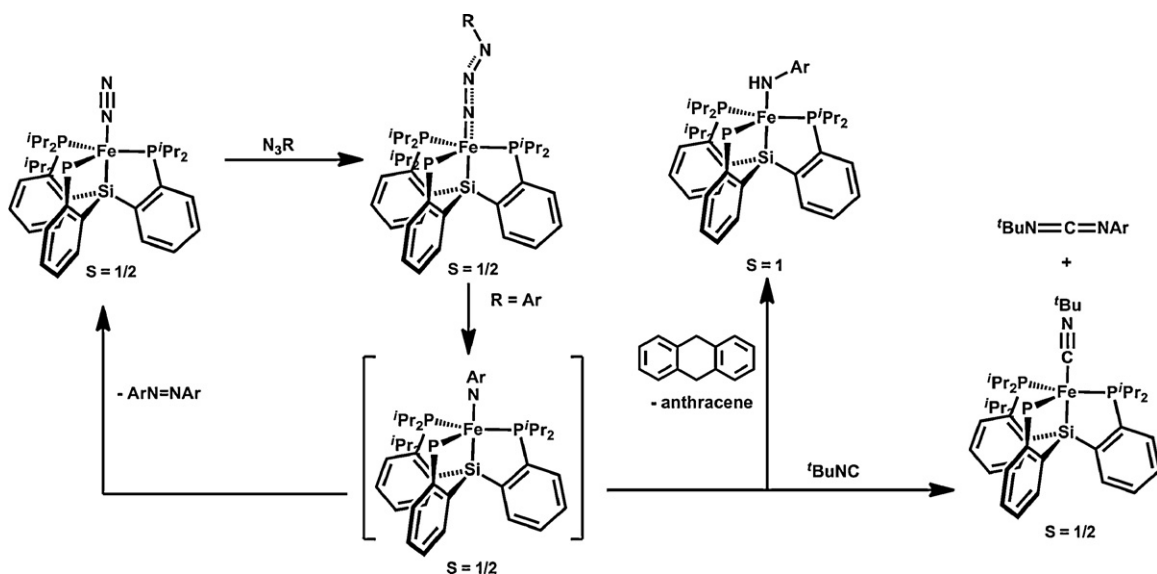
Scheme 11.

symmetry was predicted in the DFT minimized $S = 1/2$ structure. The low-spin configuration seems to be energetically preferred *in silico*, but was not appreciably lower in energy than the intermediate-spin $S = 3/2$ species, which also shows a distortion from three-fold symmetry. For comparison, a ruthenium congener, $(SiP^{iPr}_3)Ru(N\text{-}p\text{-trifluoromethylphenyl})$, could be prepared, isolated, and thoroughly characterized, including XRD analysis [139]. However, its EPR spectrum suggested an electronic structure distinct from that of $(SiP^{iPr}_3)Fe(N\text{-}p\text{-tolyl})$, and combined with accompanying X-ray data and DFT calculations, indicated that $(SiP^{iPr}_3)Ru(N\text{-}p\text{-trifluoromethylphenyl})$ is best described as a ruthenium(II) species with an imidyl radical. This may account for its enhanced stability relative to $(SiP^{iPr}_3)Fe(NAr)$.

Very recently our group has explored a ligand closely related to $(SiP^{iPr}_3)^-$, but where the Si-atom is replaced by a B-atom. The tris(phosphino)borane ligand $(2\text{-}^iPr_2PC_6H_4)_3B$, was originally introduced by Bourissou and co-workers [140], and has been abbreviated as TPB (not to be confused with TBP!). We adopt the same convention here. The tris(phosphino)borane TPB ligand might better accommodate the terminal Fe(NR) linkage due to its ability to undergo an axial distortion that would weaken the Fe–B interaction, akin to that observed by Meyer in the tris(carbene)amine ligand scaffold. While studies of (TPB)Fe species are in their early days in our labs, we have determined that the complexes $\{(TPB)Fe(N_2)\}^-$ and $(TPB)Fe(N\text{-}p\text{-MeO-phenyl})$ can be prepared (Scheme 12) and structurally characterized, and that the Fe-to-B bond distance adjusts dramatically to accommodate a π-acidic N_2 ligand (2.29 Å in $\{(TPB)Fe(N_2)\}\{Na(12\text{-crown-}4)_2\}$) relative to a π-basic imide ligand (2.61 Å in $(TPB)Fe(N\text{-}p\text{-MeO-phenyl})$). Indeed, the latter species is perhaps best formulated as trigonal pyramidal, as the iron sits 0.68 Å above the plane defined by the three phosphine donor ligands. However, a weak Fe–B interaction is indicated by DFT analysis and the triarylborane framework remains pyramidalized in the structure of $(TPB)Fe(N\text{-}p\text{-MeO-phenyl})$. The iron imide functionality displays similar metrical parameters in the solid-state (Fe–N: 1.668 Å, Fe–N–C: 170.2°) to $L_3Fe(NR)$ species in rigorously 4-coordinate geometries [141].

3.3. Trigonal bipyramidal $L'L_3Fe(CR)$ and $L'L_3Fe(N_2R)$ species

An alternative means of stabilizing metal-to-ligand multiple bonding in complexes of the $L'L_3Fe(E)$ structure type concerns coordination of a Lewis-acid (e.g., $SiMe_3^+$) to a π-acidic ligand (N_2 or CO), which should in turn enhance its π-acceptor character. This is well-illustrated by our group's recent characterization of the terminal carbyne complex $(SiP^{iPr}_3)Fe(C\text{-OSiMe}_3)$, generated via silylation of the coordinated CO ligand in $(SiP^{iPr}_3)Fe(CO)^-$ (Scheme 13) [142]. X-ray, Mössbauer, and DFT analysis of this carbyne have established that the iron center is best described as d^8 with two electron pairs strongly backdonating into the carbyne C-atom to afford an Fe–C bond distance of 1.67 Å. The one caveat to this d^8 assignment concerns the presence of a filled Fe–Si σ bonding orbital within the d-orbital energy manifold. This orbital is not shown in Fig. 2, but if included, suggests that a d^{10} assignment is also plausible. Regardless, in contrast to the Fe–N interaction in the imide species $(SiP^{iPr}_3)Fe(N\text{-}p\text{-tolyl})$, the Fe–C interaction in $(SiP^{iPr}_3)Fe(COSiMe_3)$ definitely has triple bond character. Hence, one way to circumvent the apparent incompatibility of a high d-electron count within the TBP framework and an axial multiply bonded ligand is to reverse the polarity of the multiply bonded ligand so that it is a π-acceptor rather than a π-donor (Fig. 7). Such a situation should thereby lead to stable complexes with high d-counts, and finds analogy in the stability of d^8 FeL_5 structure types such as $Fe(CO)_5$ [74].

Using a similar synthetic strategy (i.e. addition of an electrophilic silyl reagent to an Fe(0) precursor), the diazenido complex $(SiP^{iPr}_3)Fe(N_2SiMe_3)$ could likewise be generated [137]. This species is isoelectronic with $(SiP^{iPr}_3)Fe(COSiMe_3)$ and also features a degree of Fe-to-N multiple bond character. The combined solid-state structure and diamagnetic ground-state, suggested that it too can be assigned a low-spin d^8 configuration.

3.4. Trigonal bipyramidal $L'L_3Fe(O)$ species

Owing to their postulated mechanistic role in non-heme oxygen activating enzymes, there has been much recent interest in the development of synthetic iron(IV) oxo model species [5,143]. The $S = 2$ high-spin ground state of the biological non-heme ferryl intermediates is presumed to contribute to their highly reactive nature [144], and biomimetic analogues that are high-spin have likewise proven comparatively difficult to generate and characterize. The first generation of synthetic non-heme iron(IV) oxo complexes that were thoroughly characterized, including X-ray crystallography, were introduced by Que and Nam and featured local C_{4v} symmetry and intermediate-spin $S = 1$ ground states [106–109]. These have
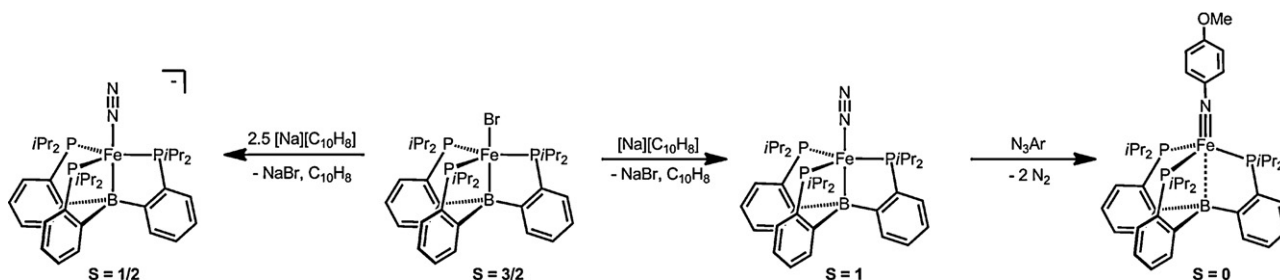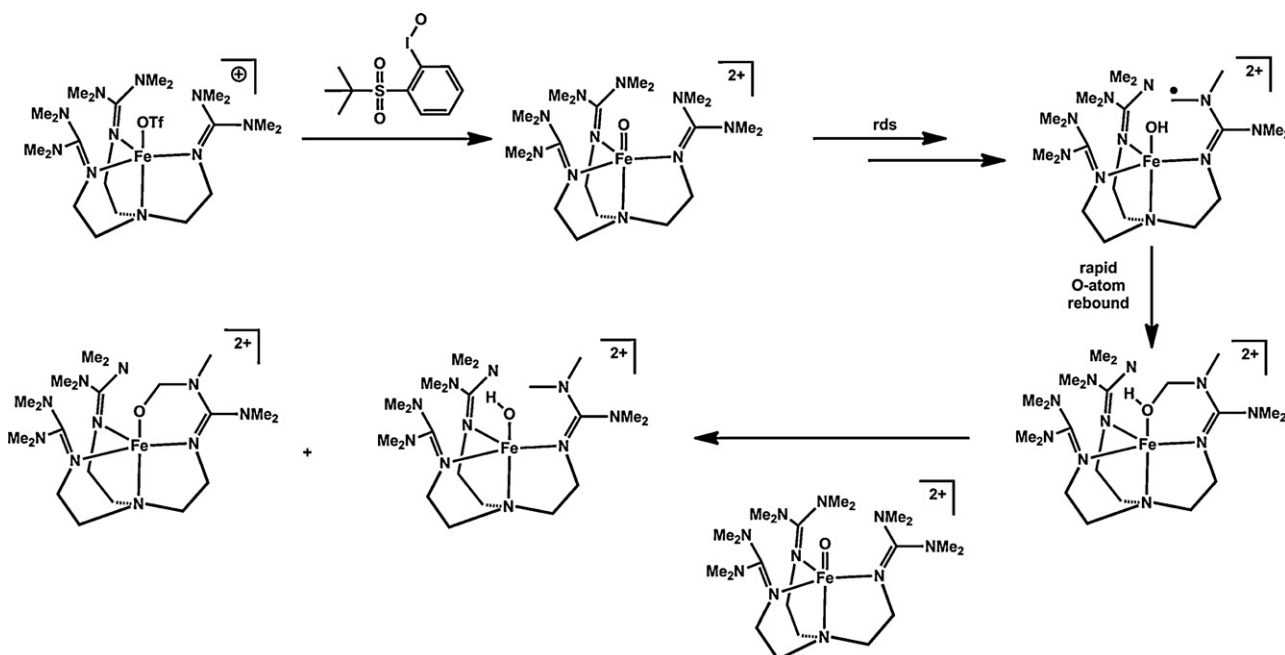
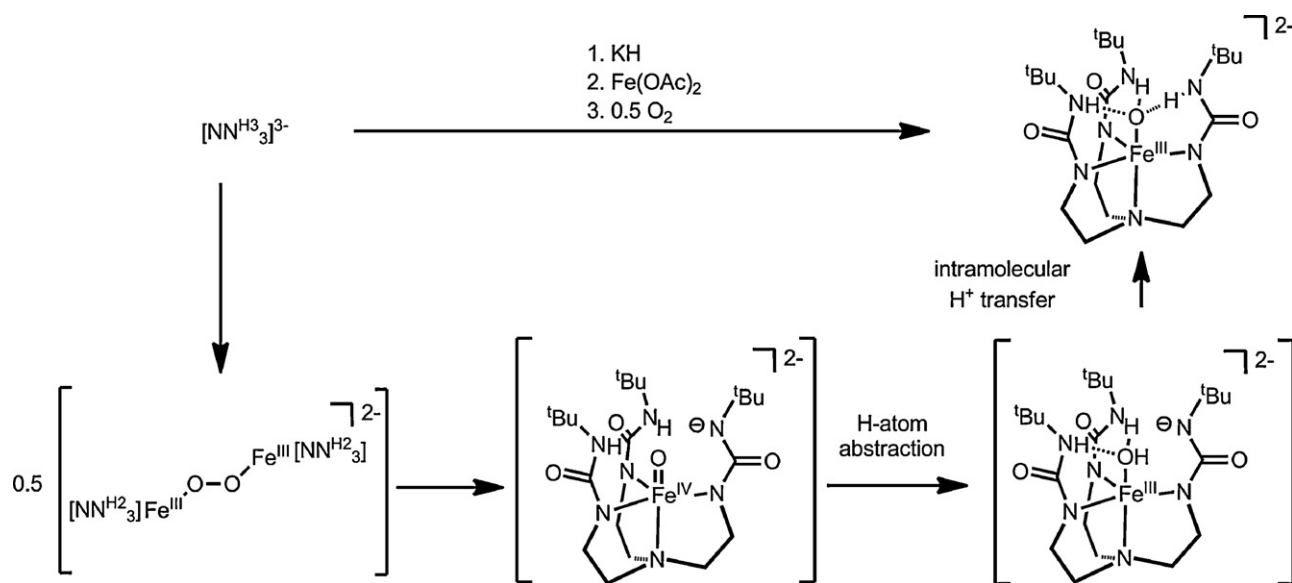**Scheme 12.**
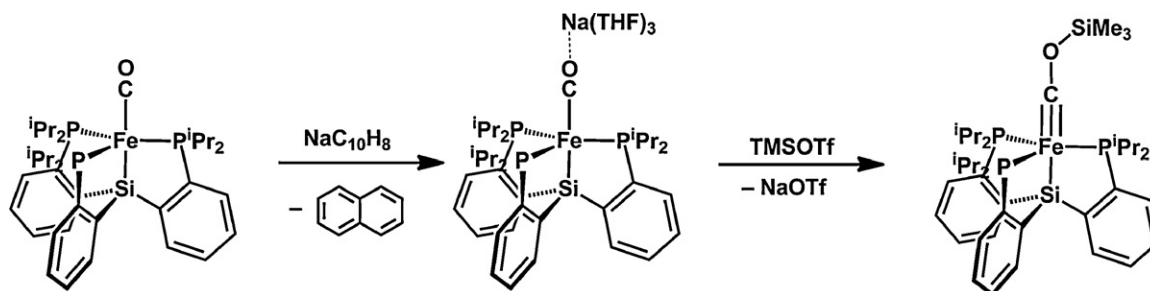
Scheme 13.

been thoroughly discussed elsewhere [8,145]. A descent from four-fold symmetry to three-fold symmetry proved necessary to access well-defined and relatively stable high-spin iron oxo species that feature Fe=O multiple bond character [146].

Que and co-workers described the preparation of the first synthetic example of a *high-spin* non-heme iron(IV) oxo species [147]. Using the neutral tetrapodal ligand TMG_3tren (TMG_3tren = 1,1,1-tris{2-[N^2-(1,1,3,3-tetramethylguanidino)]ethyl}amine), the trigonal bipyramidal precursor species $(TMG_3tren)Fe^{II}(OTf)^+$ was exploited. Treatment of $(TMG_3tren)Fe^{II}(OTf)^+$ with 2-(*tert*-butylsulfonyl)-iodosylbenzene resulted in the formation of the unusual terminal oxo species $(TMG_3tren)Fe^{IV}(O)^{2+}$ (Scheme 14). Its high-spin state was determined by Mössbauer spectroscopy, and

further corroborated by XAS and DFT calculations. The high-spin nature of $(TMG_3tren)Fe^{IV}(O)^{2+}$ appeared to contribute to its high degree of thermal instability. A facile intra-molecular self-decay pathway afforded it a half-life of only ca. 30 s at 25 °C [148]. The self-decay pathway was thoroughly examined, and the proposed mechanism of decay is shown in Scheme 14. Kinetic studies on the decay of $(TMG_3tren)Fe^{IV}(O)^{2+}$ and $(d_{36}\text{-}TMG_3tren)Fe^{IV}(O)^{2+}$ revealed a large and primary KIE of 24 at 25 °C. This isotope effect lent added stability to the deuterated analogue, and allowed for crystals suitable for X-ray data collection to be obtained at −80 °C. The Fe–O bond distance in $(d_{36}\text{-}TMG_3tren)Fe^{IV}(O)^{2+}$ was found to be 1.661(2) Å, in agreement with that predicted by DFT and the distance obtained by EXAFS. This bond distance is very similar to
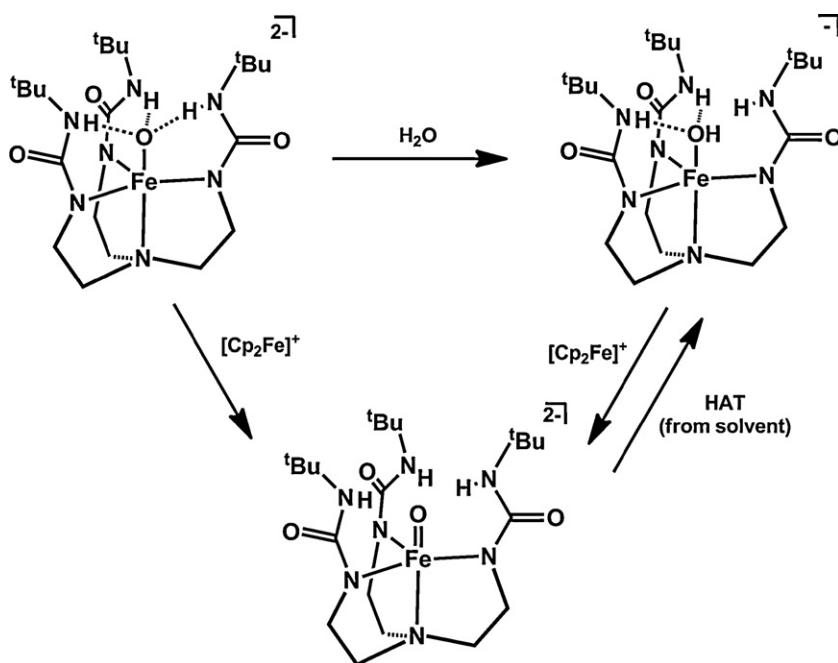

Scheme 14.

Scheme 15.

that of $S=1$ Fe=O species [56,107,149]. Taking into account the different d-orbital splitting diagrams under C_{4v} and C_{3v} symmetry this is to be expected, as in both cases the π^* orbitals are populated by only two electrons.

The group of Borovik has also been able to prepare and isolate 5-coordinate high-spin iron(IV) and iron(III) oxo complexes that reside in local three-fold symmetric environments. With the idea that H-bonding to a terminal oxo ligand may stabilize it, the trianionic, tetrapodal ligand, tris[(N′-tert-butylureaylato)-N-ethyl]aminato ([NN$^{H3}_3$]$^{3-}$) (where H3 indicates the number of H-bond donors), was developed [150]. This ligand scaffold enforces a TBP geometry, and features three acidic C(O)NH(tBu) groups above the plane of the anionic nitrogen donors, which can act as H-bond donors to an oxo ligand.

Treatment of the ligand, [NN$^{H3}_3$]$^{3-}$ with an equivalent of KH, followed by treatment with Fe(OAc)$_2$ and half an equivalent of

O$_2$, afforded the terminal oxo [NN$^{H3}_3$]Fe^{III}(O)$^{2-}$ [151]. Its proposed mechanism of formation is shown in Scheme 15, which accounts for the additional equivalent of base. This complex is remarkable in that it is high-spin, and yet relatively stable. The solid-state structure of [NN$^{H3}_3$]Fe^{III}(O)$^{2-}$ revealed that the oxo ligand is only 0.04 Å displaced from the plane defined by the three urea nitrogen atoms and is supported by H-bonding. The Fe–O bond distance of 1.813(3) Å in [NN$^{H3}_3$]Fe^{III}(O)$^{2-}$ is comparable to those found in Fe$^{III}_2$(μ-O) complexes [152], and hence is consistent with partial multiple bond character. This bond distance is however longer than that found in the d^2 [FeO$_4$]$^{2-}$, which features Fe–O bond distances that range from 1.660(2) to 1.671(2) Å [153]. The stability of [NN$^{H3}_3$]Fe^{III}(O)$^{2-}$ is in part due to the formation of hydrogen bonds, which decreases the covalency in the Fe–O bond and results in elongation of the Fe–O bond [154].
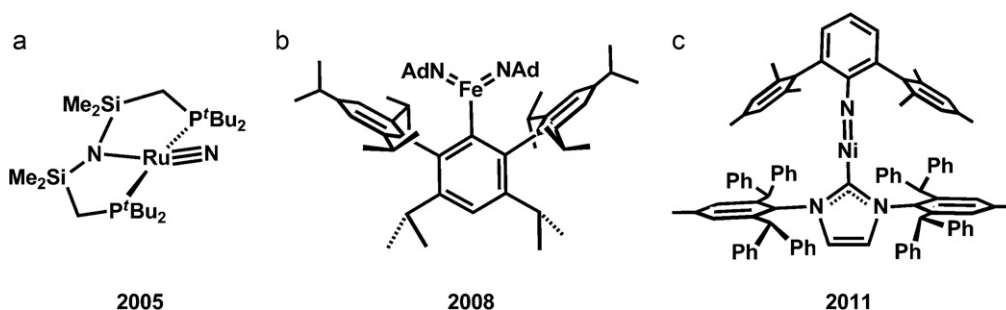

Scheme 16.

Fig. 8. Select examples of M(E) species with low coordination numbers. (a) [(^{t}Bu$_2$PCH$_2$SiMe$_2$)$_2$N]Ru^{IV}N [157], (b) (Ar)Fe^V(NAd)$_2$ [46], (c) (IAr)Ni^{II}(NAr*) [158].

The iron(III) oxo species displayed modest HAT reactivity to give [NN$^{H3}_3$]Fe^{II}(OH)$^{2-}$, though the acidity of [NN$^{H3}_3$]Fe^{III}(OH)$^-$ allowed for facile protonation as an alternative reaction pathway [155]. Both the iron(III) oxo and the hydroxo species underwent oxidation with [Cp$_2$Fe]$^+$ to generate the $S=2$ [NN$^{H3}_3$]Fe^{IV}(O)$^-$ (Scheme 16) [156]. This latter species was not thermally stable, and underwent H-atom abstraction from solvent to give [NN$^{H3}_3$]Fe^{III}(OH)$^-$ at room temperature, with a half-life of ca. 2.2 h. The strong NH bond dissociation energy of the urea nitrogen atoms likely precluded intramolecular degradation pathways, which resulted in heightened stability compared to (TMG$_3$tren)Fe^{IV}(O)$^{2+}$. The solid-state structure of [NN$^{H3}_3$]Fe^{IV}(O)$^-$ was obtained, and showed several discernable differences from its reduced congener. Now, the Fe–O bond distance has decreased by ca. 0.13 Å to 1.680(1) Å, which suggests a similar bonding description to that of (TMG$_3$tren)Fe^{IV}(O)$^{2+}$ (i.e. two electron population of π^* orbitals). The oxo ligand is 0.262 Å displaced from the plane defined by the three urea H-bonding nitrogen atoms, and combined vibrational spectroscopy and DFT calculations corroborate the absence of H-bond interactions with the oxo moiety [154,156].

4. Concluding remarks

As is hopefully now evident, the field of mid-to-late transition metals that feature metal-to-ligand multiple bonds has emerged as a rich and exciting area of coordination chemistry over the past decade. While the scope of this review has been limited to systems of iron and cobalt that reside in local three-fold symmetry, owing to our own specific expertise and research interests, mid-to-late metals in a host of local geometries and coordination numbers (e.g., linear 2-coordinate, C_{2v} 3-coordinate, C_{4v} 5- and 6-coordinate) have now been demonstrated to be compatible with metal-to-ligand multiple bonds to terminal imides, oxos, and nitrides. Fig. 8 displays a few select examples from the recent literature.

Pseudotetrahedral iron and cobalt systems of local three-fold symmetry have proven pedagogically informative in establishing how rich the redox chemistry of the L$_3$M(E) structural unit can be. Species of the type L$_3$Co^{II}(X) and L$_3$Co^{III}(E) established the feasibility of accessing d^7 and d^6 species in pseudotetrahedral low-spin environments, and suggested the more general possibility of stabilizing the M≡E linkage for mid-to-late first row ions in 4-coordinate pseudotetrahedral geometries. This possibility has been broadly realized for the case of iron. Indeed, if one considers pseudotetrahedral complexes of the type L$_3$Fe(NR) and L$_3$Fe(N), one can now find representative complexes in the formal oxidation states Fe(2+), Fe(3+), Fe(4+), and Fe(5+) in which a *bona fide* Fe≡N$_x$ triple bond is maintained (Fig. 2). These complexes constitute four spectroscopically distinct d-electron configurations. If one disrupts the π manifold by replacing the N$_x$ ligand by a chemically distinct L donor (e.g., N$_2$, PMe$_3$) then one can also access Fe(1+) (e.g., [PhBP$_3$]Fe(PMe$_3$)) and even Fe(0) (e.g., {[PhBP$_3$]Fe(N$_2$)}$^-$) as spectroscopically distinct species with different d-orbital pictures (d^7

and d^8, respectively). The lesson is a simple one. A pseudotetrahedral L$_3$Fe–X center can span six formal oxidation states, with six unique d-orbital electronic structures, simply by varying the identity of X! If one visits iron centers of higher coordination number, one now finds examples of Fe(4+), Fe(5+), and even Fe(6+). Once again, the d-orbital structures of these species are rich in terms of the spin-states that are compatible with multiply bonded ligands. The overall conclusion is at this stage clear. Whereas a decade ago the chemistry of well-defined iron complexes featuring *bona fide* and terminally bonded imides, oxos, and nitrides was in its infancy, this area of chemistry, which now spans every oxidation state from Fe(2+) to Fe(6+) and also a host of electronic states ranging from low- to intermediate- to high-spin configurations, is as rich and perhaps even richer in terms of electronic diversity than that of any other transition element.

References

[1] W.A. Nugent, J.M. Mayer, Metal Ligand Multiple Bonds, Wiley & Sons, New York, NY, 1988.
[2] R.H. Holm, J.M. Berg, Acc. Chem. Res. 19 (1986) 363–370.
[3] M.P. Doyle, Chem. Rev. 86 (1986) 919–939.
[4] J.T. Groves, Y.-Z. Han, in: P.R. Ortiz de Montellano (Ed.), Cytochrome P450: Structure, Mechanism, and Biochemistry, Plenum Press, New York, NY, 1995, pp. 3–48.
[5] M. Costas, M.P. Mehn, M.P. Jensen, L. Que, Chem. Rev. 104 (2004) 939–986.
[6] M.P. Mehn, J.C. Peters, J. Inorg. Biochem. 100 (2006) 634–643.
[7] M.T. Green, Curr. Opin. Chem. Biol. 13 (2009) 84–88.
[8] L. Que, Acc. Chem. Res. 40 (2007) 493–500.
[9] J.P. Collman, X.M. Zhang, V.J. Lee, E.S. Uffelman, J.I. Brauman, Science 261 (1993) 1404–1411.
[10] Y. Gao, R.M. Hanson, J.M. Klunder, S.Y. Ko, H. Masamune, K.B. Sharpless, J. Am. Chem. Soc. 109 (1987) 5765–5780.
[11] K.A. Joergensen, Chem. Rev. 89 (1989) 431–458.
[12] J.T. Groves, T. Takahashi, J. Am. Chem. Soc. 105 (1983) 2073–2074.
[13] Z. Li, R.W. Quan, E.N. Jacobsen, J. Am. Chem. Soc. 117 (1995) 5889–5890.
[14] D.A. Evans, K.A. Woerpel, M.M. Hinman, M.M. Faul, J. Am. Chem. Soc. 113 (1991) 726–728.
[15] P. Müller, C. Fruit, Chem. Rev. 103 (2003) 2905–2919.
[16] H.M.L. Davies, T. Hansen, M.R. Churchill, J. Am. Chem. Soc. 122 (2000) 3063–3070.
[17] H.M.L. Davies, J.R. Manning, Nature 451 (2008) 417–424.
[18] A. Gunay, K.H. Theopold, Chem. Rev. 110 (2010) 1060–1081.
[19] J. Rittle, M.T. Green, Science 330 (2010) 933–937.

[20] R.R. Schrock, Acc. Chem. Res. 38 (2005) 955–962.
[21] J.L. Crossland, D.R. Tyler, Coord. Chem. Rev. 254 (2010) 1883–1894.
[22] S. Shaik, H. Hirao, D. Kumar, Acc. Chem. Res. 40 (2007) 532–542.
[23] S. Shaik, W. Lai, H. Chen, Y. Wang, Acc. Chem. Res. 43 (2010) 1154–1165.
[24] T.R. Cundari, A. Dinescu, A.B. Kazi, Inorg. Chem. 47 (2008) 10067–10072.
[25] T.R. Cundari, J. Am. Chem. Soc. 114 (1992) 7879–7888.
[26] T.A. Betley, Q. Wu, T. Van Voorhis, D.G. Nocera, Inorg. Chem. 47 (2008) 1849–1861.
[27] J.F. Berry, Comment. Inorg. Chem. 30 (2009) 28–66.
[28] C.J. Ballhausen, H.B. Gray, Inorg. Chem. 1 (1962) 111–122.
[29] J.M. Mayer, Inorg. Chem. 27 (1988) 3899–3903.
[30] C.C. Cummins, R.R. Schrock, W.M. Davis, Organometallics 11 (1992) 1452–1454.
[31] A.L. Odom, C.C. Cummins, J.D. Protasiewicz, J. Am. Chem. Soc. 117 (1995) 6613–6614.
[32] T.M. Anderson, W.A. Neiwert, M.L. Kirk, P.M.B. Piccoli, A.J. Schultz, T.F. Koetzle, D.G. Musaev, K. Morokuma, R. Cao, C.L. Hill, Science 306 (2004) 2074–2077.
[33] J.M. Mayer, T.H. Tulip, J. Am. Chem. Soc. 106 (1984) 3878–3879.
[34] J.M. Mayer, Comment. Inorg. Chem. 8 (1988) 125–135.
[35] E. Spaltenstein, R.R. Conry, S.C. Critchlow, J.M. Mayer, J. Am. Chem. Soc. 111 (1989) 8741–8742.
[36] G. Rouschias, Chem. Rev. 74 (1974) 531–566.
[37] J.M. Mayer, D.L. Thorn, T.H. Tulip, J. Am. Chem. Soc. 107 (1985) 7454–7462.
[38] B.A. Moyer, T.J. Meyer, Inorg. Chem. 20 (1981) 436–444.
[39] B.A. Moyer, T.J. Meyer, J. Am. Chem. Soc. 100 (1978) 3601–3603.
[40] M.S. Thompson, T.J. Meyer, J. Am. Chem. Soc. 104 (1982) 4106–4115.
[41] D.S. Glueck, J.X. Wu, F.J. Hollander, R.G. Bergman, J. Am. Chem. Soc. 113 (1991) 2041–2054.
[42] R.S. Haymotherwell, G. Wilkinson, B. Hussainbates, M.B. Hursthouse, Polyhedron 12 (1993) 2009–2012.
[43] M.P. Jensen, M.P. Mehn, L. Que (Eds.), Angew. Chem. Int. Ed. 42 (2003) 4357–4360.
[44] E.R. King, T.A. Betley, Inorg. Chem. 48 (2009) 2361–2363.
[45] R.L. Lucas, D.R. Powell, A.S. Borovik, J. Am. Chem. Soc. 127 (2005) 11596–11597.
[46] C. Ni, J.C. Fettinger, G.J. Long, M. Brynda, P.P. Power, Chem. Commun. (2008) 6045–6047.
[47] S.C. Bart, E. Lobkovsky, E. Bill, P.J. Chirik, J. Am. Chem. Soc. 128 (2006) 5302–5303.
[48] J.J. Scepaniak, J.A. Young, R.P. Bontchev, J.M. Smith (Eds.), Angew. Chem. Int. Ed. 48 (2009) 3158–3160.
[49] J.J. Scepaniak, M.D. Fulton, R.P. Bontchev, E.N. Duesler, M.L. Kirk, J.M. Smith, J. Am. Chem. Soc. 130 (2008) 10515–10517.
[50] I. Nieto, F. Ding, R.P. Bontchev, H.B. Wang, J.M. Smith, J. Am. Chem. Soc. 130 (2008) 2716–2717.
[51] C. Vogel, F.W. Heinemann, J. Sutter, C. Anthon, K. Meyer (Eds.), Angew. Chem. Int. Ed. 47 (2008) 2681–2684.
[52] T.A. Betley, J.C. Peters, J. Am. Chem. Soc. 126 (2004) 6252–6254.
[53] S.D. Brown, T.A. Betley, J.C. Peters, J. Am. Chem. Soc. 125 (2003) 322–323.
[54] S.D. Brown, J.C. Peters, J. Am. Chem. Soc. 127 (2005) 1913–1923.
[55] C.M. Thomas, N.P. Mankad, J.C. Peters, J. Am. Chem. Soc. 128 (2006) 4956–4957.
[56] J.-U. Rohde, J.H. In, M.H. Lim, W.W. Brennessel, M.R. Bukowski, A. Stubna, E. Münck, W. Nam, L. Que, Science 299 (2003) 1037–1039.
[57] D.M. Jenkins, T.A. Betley, J.C. Peters, J. Am. Chem. Soc. 124 (2002) 11238–11239.
[58] X. Hu, K. Meyer, J. Am. Chem. Soc. 126 (2004) 16322–16323.
[59] R.E. Cowley, R.P. Bontchev, J. Sorrell, O. Sarracino, Y.H. Feng, H.B. Wang, J.M. Smith, J. Am. Chem. Soc. 129 (2007) 2424–2425.
[60] X.L. Dai, P. Kapoor, T.H. Warren, J. Am. Chem. Soc. 126 (2004) 4798–4799.
[61] E. Kogut, H.L. Wiencko, L.B. Zhang, D.E. Cordeau, T.H. Warren, J. Am. Chem. Soc. 127 (2005) 11248–11249.
[62] D.J. Mindiola, G.L. Hillhouse, J. Am. Chem. Soc. 123 (2001) 4623–4624.
[63] R. Melenkivitz, D.J. Mindiola, G.L. Hillhouse, J. Am. Chem. Soc. 124 (2002) 3846–3847.
[64] D.J. Mindiola, G.L. Hillhouse, J. Am. Chem. Soc. 124 (2002) 9976–9977.
[65] N.A. Eckert, S. Vaddadi, S. Stoian, R.J. Lachicotte, T.R. Cundari, P.L. Holland (Eds.), Angew. Chem. Int. Ed. 45 (2006) 6868–6871.
[66] R.E. Cowley, N.J. DeYonker, N.A. Eckert, T.R. Cundari, S. DeBeer, E. Bill, X. Ottenwaelder, C. Flaschenriem, P.L. Holland, Inorg. Chem. 49 (2010) 6172–6187.
[67] R.E. Cowley, N.A. Eckert, J. Elhaïk, P.L. Holland, Chem. Commun. (2009) 1760–1762.
[68] P.L. Holland, Acc. Chem. Res. 41 (2008) 905–914.
[69] D.M. Jenkins, A.J. Di Bilio, M.J. Allen, T.A. Betley, J.C. Peters, J. Am. Chem. Soc. 124 (2002) 15336–15350.
[70] D.M. Jenkins, J.C. Peters, J. Am. Chem. Soc. 125 (2003) 11162–11163.
[71] D.M. Jenkins, J.C. Peters, J. Am. Chem. Soc. 127 (2005) 7148–7165.
[72] I.R. Shapiro, D.M. Jenkins, J.C. Thomas, M.W. Day, J.C. Peters, Chem. Commun. (2001) 2152–2153.
[73] T.A. Betley, J.C. Peters, J. Am. Chem. Soc. 125 (2003) 10782–10783.
[74] F.A. Cotton, G. Wilkinson, Advanced Inorganic Chemistry, 5th ed., Wiley, New York, 1988.
[75] B.B. Garrett, V.L. Goedken, J.V. Quaglian, J. Am. Chem. Soc. 92 (1970) 489.
[76] M. Gerloch, L.R. Hanton, Inorg. Chem. 19 (1980) 1692–1698.
[77] M. Gerloch, M.R. Manning, Inorg. Chem. 20 (1981) 1051–1056.
[78] L. Banci, C. Benelli, D. Gatteschi, F. Mani, Inorg. Chem. 21 (1982) 1133–1136.

[79] H.B. Gray, Chemical Bonds: An Introduction to Atomic and Molecular Structure, University Science Books, Mill Valley, CA, 1994.
[80] S.H. Strauss, M.E. Silver, K.M. Long, R.G. Thompson, R.A. Hudgens, K. Spartalian, J.A. Ibers, J. Am. Chem. Soc. 107 (1985) 4207–4215.
[81] V.L. Goedken, J.J. Pluth, S.-M. Peng, B. Bursten, J. Am. Chem. Soc. 98 (1976) 8014–8021.
[82] T.A. Betley, J.C. Peters, Inorg. Chem. 42 (2003) 5074–5084.
[83] T.A. Albright, J.K. Burdett, M.H. Whangbo, Orbital Interactions in Chemistry, John Wiley & Sons, New York, 1985.
[84] A.K. Verma, T.N. Nazif, C. Achim, S.C. Lee, J. Am. Chem. Soc. 122 (2000) 11013–11014.
[85] M.P. Mehn, S.D. Brown, D.M. Jenkins, J.C. Peters, L. Que, Inorg. Chem. 45 (2006) 7417–7427.
[86] G.P.A. Yap, CCDC Deposition Number 253991, 2004.
[87] D.T. Shay, G.P.A. Yap, L.N. Zakharov, A.L. Rheingold, K.H. Theopold (Eds.), Angew. Chem. Int. Ed. 44 (2005) 1508–1510.
[88] I.H. Wasbotten, A. Ghosh, Inorg. Chem. 46 (2007) 7890–7898.
[89] N.P. Mankad, P. Müller, J.C. Peters, J. Am. Chem. Soc. 132 (2010) 4083–4084.
[90] D.J. Mindiola, G.L. Hillhouse, Chem. Commun. (2002) 1840–1841.
[91] D.T. Shay, G.P.A. Yap, L.N. Zakharov, A.L. Rheingold, K.H. Theopold (Eds.), Angew. Chem. Int. Ed. 45 (2006) 7870–17870.
[92] S. Thyagarajan, D.T. Shay, C.D. Incarvito, A.L. Rheingold, K.H. Theopold, J. Am. Chem. Soc. 125 (2003) 4440–4441.
[93] I. Nieto, F. Cervantes-Lee, J.M. Smith, Chem. Commun. (2005) 3811–3813.
[94] A.K. Burred, A.J. Steedman, J. Chem. Soc., Chem. Commun. (1995) 2109–2110.
[95] A.A. Danopoulos, G. Wilkinson, B. Hussain-Bates, M.B. Hursthouse, Polyhedron 11 (1992) 2961–2964.
[96] B. Bell, J. Chatt, J.R. Dilworth, G.J. Leigh, Inorg. Chim. Acta 6 (1972) 635–637.
[97] R.I. Michelman, R.A. Andersen, R.G. Bergman, J. Am. Chem. Soc. 113 (1991) 5100–5102.
[98] C.C. Lu, C.T. Saouma, M.W. Day, J.C. Peters, J. Am. Chem. Soc. 129 (2007) 4–5.
[99] J.L. Kisko, T. Hascall, G. Parkin, J. Am. Chem. Soc. 120 (1998) 10561–10562.
[100] M.F. Lappert, J.J. MacQuitty, P.L. Pye, J. Chem. Soc., Dalton Trans. (1981) 1583–1592.
[101] Y.S. Sohn, D.N. Hendrickson, H.B. Gray, J. Am. Chem. Soc. 92 (1970) 3233–3234.
[102] Y.S. Sohn, D.N. Hendrickson, H.B. Gray, J. Am. Chem. Soc. 93 (1971) 3603–3612.
[103] S.D. Brown, J.C. Peters, J. Am. Chem. Soc. 126 (2004) 4538–4539.
[104] E.J. Daida, J.C. Peters, Inorg. Chem. 43 (2004) 7474–7485.
[105] Y.S. Sohn, D.N. Hendrickson, J. Hart Smith, H.B. Gray, Chem. Phys. Lett. 6 (1970) 499–501.
[106] T.K. Paine, M. Costas, J. Kaizer, L. Que, J. Biol. Inorg. Chem. 11 (2006) 272–276.
[107] E.J. Klinker, J. Kaizer, W.W. Brennessel, N.L. Woodrum, C.J. Cramer, L. Que (Eds.), Angew. Chem. Int. Ed. 44 (2005) 3690–3694.
[108] J.-U. Rohde, S. Torelli, X.P. Shan, M.H. Lim, E.J. Klinker, J. Kaizer, K. Chen, W.W. Nam, L. Que, J. Am. Chem. Soc. 126 (2004) 16750–16761.
[109] M.H. Lim, J.-U. Rohde, A. Stubna, M.R. Bukowski, M. Costas, R.Y.N. Ho, E. Münck, W. Nam, L. Que, Proc. Natl. Acad. Sci. U.S.A. 100 (2003) 3665–3670.
[110] J.C. Thomas, J.C. Peters, Inorg. Chem. 42 (2003) 5055–5073.
[111] D.E. Fjare, W.L. Gladfelter, Inorg. Chem. 20 (1981) 3533–3539.
[112] M.V. Bennett, S. Stoian, E.L. Bominaar, E. Münck, R.H. Holm, J. Am. Chem. Soc. 127 (2005) 12378–12386.
[113] D.A. Summerville, I.A. Cohen, J. Am. Chem. Soc. 98 (1976) 1747–1752.
[114] M. Li, M. Shang, N. Ehlinger, C.E. Schulz, W.R. Scheidt, Inorg. Chem. 39 (2000) 580–583.
[115] W.D. Wagner, K. Nakamoto, J. Am. Chem. Soc. 110 (1988) 4044–4045.
[116] W.D. Wagner, K. Nakamoto, J. Am. Chem. Soc. 111 (1989) 1590–1598.
[117] K. Meyer, E. Bill, B. Mienert, T. Weyhermüller, K. Wieghardt, J. Am. Chem. Soc. 121 (1999) 4859–4876.
[118] M. Aliaga-Alcalde, S.D. George, B. Mienert, E. Bill, K. Wieghardt, F. Neese (Eds.), Angew. Chem. Int. Ed. 44 (2005) 2908–2912.
[119] J.F. Berry, E. Bill, E. Bothe, S.D. George, B. Mienert, F. Neese, K. Wieghardt, Science 312 (2006) 1937–1941.
[120] J.F. Berry, S. DeBeer George, F. Neese, Phys. Chem. Chem. Phys. 10 (2008) 4361–4374.
[121] J. Du Bois, C.S. Tomooka, J. Hong, E.M. Carreira, Acc. Chem. Res. 30 (1997) 364–372.
[122] C.J. Chang, D.W. Low, H.B. Gray, Inorg. Chem. 36 (1997) 270–271.
[123] T. Petrenko, S.D. George, N. Aliaga-Alcalde, E. Bill, B. Mienert, Y. Xiao, Y. Guo, W. Sturhahn, S.P. Cramer, K. Wieghardt, F. Neese, J. Am. Chem. Soc. 129 (2007) 11053–11060.
[124] D.J. Mindiola, C.C. Cummins (Eds.), Angew. Chem. Int. Ed. 37 (1998) 945–947.
[125] C.C. Lu, J.C. Peters, Inorg. Chem. 45 (2006) 8597–8607.
[126] C.E. MacBeth, J.C. Thomas, T.A. Betley, J.C. Peters, Inorg. Chem. 43 (2004) 4645–4662.
[127] J.C. Peters, A.R. Johnson, A.L. Odom, P.W. Wanandi, W.M. Davis, C.C. Cummins, J. Am. Chem. Soc. 118 (1996) 10175–10188.
[128] C.E. Laplaza, C.C. Cummins, Science 268 (1995) 861–863.
[129] D.V. Yandulov, R.R. Schrock, J. Am. Chem. Soc. 124 (2002) 6252–6253.
[130] K. Nakamoto, Infrared and Raman Spectra of Inorganic and Coordination Compounds Part B: Applications in Coordination, Organometallic, and Bioinorganic Chemistry, 5th ed., John Wiley & Sons, Inc, New York, 1997.
[131] M.P. Hendrich, W. Gunderson, R.K. Behan, M.T. Green, M.P. Mehn, T.A. Betley, C.C. Lu, J.C. Peters, Proc. Natl. Acad. Sci. U.S.A. 103 (2006) 17107–17112.
[132] J.-U. Rohde, T.A. Betley, T.A. Jackson, C.T. Saouma, J.C. Peters, L. Que Jr., Inorg. Chem. 46 (2007) 5720–5726.

[133] J.J. Scepaniak, C.A. Vogel, M.M. Khusniyarov, F.W. Heinemann, K. Meyer, J.M. Smith, Science, in press (2011).
[134] V.M. Miskowski, H.B. Gray, M.D. Hopkins, Adv. Transit. Met. Coord. Chem. 1 (1996) 159–186.
[135] M.T. Whited, N.P. Mankad, Y.H. Lee, P.F. Oblad, J.C. Peters, Inorg. Chem. 48 (2009) 2507–2517.
[136] N.P. Mankad, M.T. Whited, J.C. Peters (Eds.), Angew. Chem. Int. Ed. 46 (2007) 5768–5771.
[137] Y.H. Lee, N.P. Mankad, J.C. Peters, Nat. Chem. 2 (2010) 558–565.
[138] N.A. Eckert, S. Vaddadi, S. Stoian, R.J. Lachicotte, T.R. Cundari, P.L. Holland, Angew. Chem. Int. Ed. 45 (2006) 6868–6871.
[139] A. Takaoka, L.C.H. Gerber, J.C. Peters (Eds.), Angew. Chem. Int. Ed. 49 (2010) 4088–4091.
[140] S. Bontemps, G. Bouhadir, P.W. Dyer, K. Miqueu, D. Bourissou, Inorg. Chem. 46 (2007) 5149–5151.
[141] M.-E. Moret, J.C. Peters, Angew. Chem. Int. Ed. in press (2011), doi:10.10021/anie.201006918.
[142] Y. Lee, J.C. Peters, J. Am. Chem. Soc. in press (2011).
[143] X. Shan, L. Que Jr, J. Inorg. Biochem. 100 (2006) 421–433.
[144] A. Decker, J.-U. Rohde, E.J. Klinker, S.D. Wong, L. Que, E.I. Solomon, J. Am. Chem. Soc. 129 (2007) 15983–15996.
[145] W. Nam, Acc. Chem. Res. 40 (2007) 522–531.
[146] O. Pestovsky, S. Stoian, E.L. Bominaar, X. Shan, E. Münck, L. Que, A. Bakac (Eds.), Angew. Chem. Int. Ed. 44 (2005) 6871–6874.
[147] J. England, M. Martinho, E.R. Farquhar, J.R. Frisch, E.L. Bominaar, E. Münck, L. Que (Eds.), Angew. Chem. Int. Ed. 48 (2009) 3622–3626.
[148] J. England, Y. Guo, E.R. Farquhar, V.G. Young Jr., E. Münck, L. Que Jr, J. Am. Chem. Soc. 132 (2010) 8635–8644.
[149] A. Thibon, J. England, M. Martinho, V.G. Young, J.R. Frisch, R. Guillot, J.-J. Girerd, E. Münck, L. Que, F. Banse (Eds.), Angew. Chem. Int. Ed. 47 (2008) 7064–7067.
[150] A.S. Borovik, Acc. Chem. Res. 38 (2005) 54–61.
[151] C.E. MacBeth, A.P. Golombek, V.G. Young, C. Yang, K. Kuczera, M.P. Hendrich, A.S. Borovik, Science 289 (2000) 938–941.
[152] D.M. Kurtz, Chem. Rev. 90 (1990) 585–606.
[153] M.L. Hoppe, E.O. Schlemper, R.K. Murmann, Acta Crystallogr. B 38 (1982) 2237–2239.
[154] A. Dey, R.K. Hocking, P. Larsen, A.S. Borovik, K.O. Hodgson, B. Hedman, E.I. Solomon, J. Am. Chem. Soc. 128 (2006) 9825–9833.
[155] R. Gupta, A.S. Borovik, J. Am. Chem. Soc. 125 (2003) 13234–13242.
[156] D.C. Lacy, R. Gupta, K.L. Stone, J. Greaves, J.W. Ziller, M.P. Hendrich, A.S. Borovik, J. Am. Chem. Soc. 132 (2010) 12188–12190.
[157] A. Walstrom, M. Pink, X.F. Yang, J. Tomaszewski, M.H. Baik, K.G. Caulton, J. Am. Chem. Soc. 127 (2005) 5330–5331.
[158] C.A. Laskowski, A.J.M. Miller, G.L. Hillhouse, T.R. Cundari, J. Am. Chem. Soc. ASAP (2011), doi:10.1021/ja1101213.